



Research paper

Optimal deployment of fast-charging stations for electric vehicles considering the sizing of the electrical distribution network and traffic condition

Miguel Campaña ^{a,b,*}, Esteban Inga ^b^a Power Grid and Alternative Energies Research Group, Master of Electricity Program, Instituto Superior Universitario Sucre, Quito EC170148, Ecuador^b Smart Grid Research Group, Master of Electricity Program, Universidad Politécnica Salesiana, Quito 170525, Ecuador

ARTICLE INFO

Article history:

Received 9 October 2022

Received in revised form 1 April 2023

Accepted 19 April 2023

Available online 1 May 2023

Keywords:

EV charging stations
 Electrical distribution networks
 Georeferenced systems
 Vehicle flow paths
 Optimization
 Capacitated Multicommodity Flow Problem
 Smart Grid
 Smart City

ABSTRACT

The conventional vehicle fleet worldwide has contributed to the degradation of air quality due to CO₂ emissions. Consequently, it has migrated from internal combustion to electric vehicles (EVs). However, it is essential to ensure the deployment of electric vehicle charging station infrastructures (EVCSI) to guarantee their interoperability for the development of electric mobility. Moreover, the sustainability of EVCSI depends not only on the capacity to meet demand but also on the adequate number of terminals in the different public charging stations (CS) to reduce waiting times for battery recharging. Then to achieve an optimal sizing of charging stations, it is crucial to foresee the maximum number of vehicles that could use the different CS during a time interval. The sizing of CS must respond to real mobility constraints and technical conditions, such as the capacity of vehicular flow, the capacity of the roads according to their geometry, the trajectories marked by the users, and the possible exit of operation of some CS. Therefore, this paper addresses the problem considering four fundamental axes, which are: stochastic analysis of heterogeneous vehicular flow, a solution to the transportation problem with the capacitated multicommodity flow problem and Hungarian algorithm, analysis of the optimal number of terminals considering loading times, and finally the proposed EVCSI will be validated using the CymDist software for electrical engineering. Consequently, the computational complexity of the model is of a combinatorial type and is defined as NP-hard given the multiple variables and constraints within the transportation problem.

© 2023 The Authors. Published by Elsevier Ltd. This is an open access article under the CC BY-NC-ND license (<http://creativecommons.org/licenses/by-nc-nd/4.0/>).

1. Introduction

Electric energy supply in charging infrastructures plays an essential role in the sustainability of this new non-conventional mobility alternative. This new mobility concept contributes directly to reducing greenhouse gases, noise, and visual pollution compared to conventional mobility. In Europe, it is estimated that approximately 80% of the noise pollution caused on the streets is generated by vehicles that use fossil fuels as a source of energy. In addition, human mobility plays a fundamental role in cities' development and economic growth. However, with conventional mobility, the environmental cost becomes critical and detrimental to future generations due to the radical climate change we are currently undergoing. The most challenging problem is the supply chain management for EV charging; therefore, planning the deployment of CS (Liu et al., 2019b) is essential. To plan,

forecast the demand, and guarantee the continuity of the electric service, it is crucial to study and simulate the theoretical vehicular flow in a georeferenced area. This way, it is possible to forecast the resources needed in each CS. It is essential to foresee the maximum demand of CS since it would help us to decide if the electrical network can assume new loads or, if not, it is necessary to create new supply circuits for each CS. It would contribute significantly to maintaining voltage stability in conventional distribution power systems and foresee the expansion of the power grid. Therefore, planning can be divided into four stages: (i) highly stochastic demand prediction, (ii) CS allocation, and sizing, (iii) minimum routing from demand to a power source to recharge the battery, and (iv) georeferenced simulation of the distribution power system that will support the charging infrastructure. Consequently, two optimizing variables are identified (i) operating costs and (ii) heterogeneous load distribution in georeferenced scenarios (Rabbani et al., 2019; Campaña et al., 2021). Finally, this paper observes a multi-objective approach to address the problems of heterogeneous vehicular traffic routing, CS sizing, and determining the optimal number of charging terminals for EVs (Asna et al., 2023).

* Correspondence to: Smart Grid Research Group, Universidad Politécnica Salesiana, Quito 170525, Ecuador.

E-mail addresses: mcampaña@tecnologicosure.edu.ec (M. Campaña), inga@ups.edu.ec (E. Inga).

Nomenclature	
List of variables	
G	Directed graph
φ	Vehicular traffic
\mathcal{V}	Vertex set
\mathcal{A}	Creation of spanning trees
V_e	# Electric vehicles
ε	Charging stations
ζ	Nodes involved in the road network
u, v	Source–destination edges respectively
ι	Track section length
ω	Traffic capacity in ι
β	Ordered pair of vertices in a track section (products))
W_β	Cost per traffic demand
$S_{1,2,3,\dots}$	Available routes on the road network
f_{beta}	Traffic flow
i, j	Indexes to relate the road network
κ	Sites selected for CS location
m	Size of vector u, v .
δ_κ	costcost, in terms of traffic as viewed from a CS
n	# Vehicles, observing capacity criteria in each road section.
ψ	Road capacity
\mathcal{M}	Subsets edges define enabled roads
\mathcal{L}	Subset of edges of a path
ϕ_j	Location variable
θ_k	Subset of assigned arcs
τ_e^j	Path enabled
np	Number of periods in years
q	Vehicle density of each commodity
α	Number of vehicles in ι
t_s	Time in hours
Θ	Annual rate of increase in the vehicle fleet
s	Vehicle spacing
Sp	Travel speed of each EV
$r(\mathcal{S})$	Reduced-cost variable
T	Indicates the transpose of the matrix
X_*^k	Optimal dual objective function
ω	Dual variable array
c	Costs
b	Inequality vector b
A	Inequality matrix A
x	Independent variable
$\pi_{1,2}$	Dual variables
$M/M/s$	Multichannel queuing model
M	# Available charging terminals
λ	Average arrival rate
μ	Average service rate in each channel
η	Number of EV units in system
W_s	Average time that an electric vehicle remains in the system
P_0	Probability
P_o	Active power when the supply voltage corresponds to 1 p.u.
Q_0	Reactive power when the power supply voltage corresponds to 1 p.u.
V_0	Voltage when the supply voltage corresponds to 1 p.u.
P	Active power model as a function of voltage variation
Q	Reactive power model as a function of voltage variation
$p_1 - p_3$	Active power parameters
$q_1 - q_3$	Reactive power parameters
V	Supply voltage at p.u.

Depending on the number of terminals to recharge EV batteries, the service time in the CS could increase or decrease significantly. In addition, the number of charging terminals for EVs may result in the need for more or more petite sizing of the electrical equipment required in the charging infrastructure. Consequently, for CS sizing, resources are allocated according to the number of EVs expected to be served in a CS hourly. Therefore, the sum of the partial demands generated by each EV must equal the resource assigned in the CS sizing problem. Candidate locations for CS include parks, shopping malls, public–private green spaces, and parking lots.

Fig. 1 presents the architecture proposed in this article. It shows a two-level spatial approach (I) demands based on vehicular flow analysis and (II) electrical equipment for charging infrastructure. These demands are met by deploying a set of CS in permitted public areas such as parking lots, parks, and high concurrency areas. In addition, the equipment for the charging infrastructure should consider forecasting vehicle demand based on the maximum traffic density generated on the road network. Consequently, the heuristic proposed in this article will solve the allocation of electric equipment in charging infrastructures, considering real transportation constraints under a spatial approach. Therefore, the objective is to solve multiple resource allocation problems in a georeferenced area of NP-hard computational complexity, relying on optimization tools, graph theory, and routing algorithms, thus reducing the computational complexity to a problem of NP type (Jiménez-Estévez et al., 2010).

1.1. Contributions and structure

Level I analyzes vehicular traffic in the road network, observing capacity and level of service criteria, allowing weights to the road network's different trajectories to enter the optimization model. However, it is noted that this is not a trivial problem, and it is a great challenge to solve, given that, in the analysis of vehicular traffic, geographical elements are involved (roads, orography, overpasses), the dispositions of the vehicles are unknown. Therefore, due to their high traffic variability, it is impossible to predict the trajectory patterns with certainty (Jiang et al., 2018; Zhang and Ioannou, 2018; Song et al., 2019). Consequently, to develop optimal routes in trajectories, it is crucial to pay special attention to aspects that have to do with the variables of vehicular flow, the probabilistic description of vehicular traffic, the distribution of vehicles in a road network, and the statistical distribution of vehicular density. In this first level, the microscopic, Hungarian, and multicommodity flow problem models are used to identify the maximum vehicular flow the road network can experience and direct the traffic to the different CS deployed in the area of interest. In addition, it is possible to determine the number of EVs that a CS can serve at the level, considering that one of them goes out of service of the charging infrastructure. The

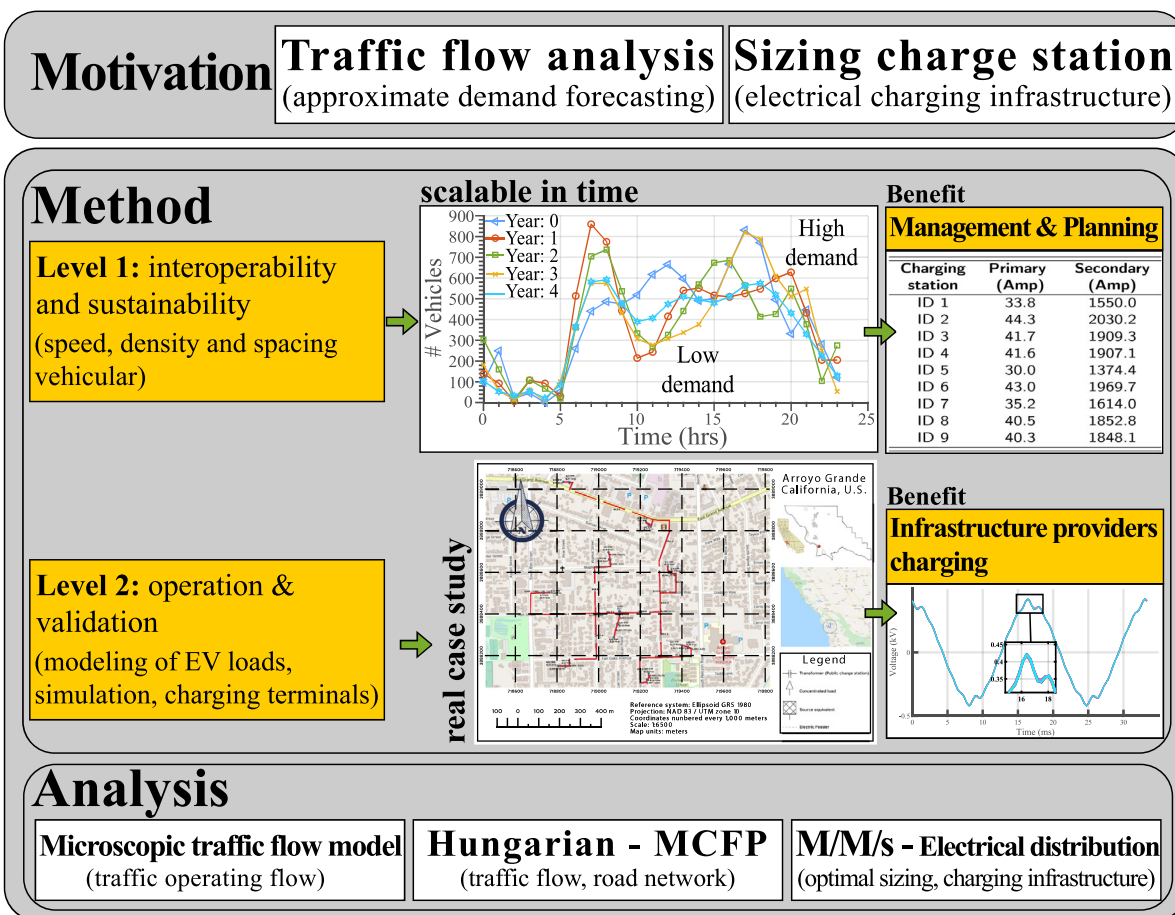


Fig. 1. Proposed architecture for the deployment of electric charging stations.

exit from service of a CS will cause the vehicular flow to be reorganized, and the demand covered by the CS that went out of service will be directed to the available CS. Considering the eventual exit of a CS is undoubtedly a significant contribution to the optimal sizing of CS and, in general, the charging infrastructure. Level II analyzes the topology generated to achieve the supply of electric power to each CS and thus meet the demand by massive introduction of EV in the vehicle flow management processes (Montoya and Ramirez, 2012; Li et al., 2014; Nagarajan and Ayyanar, 2014; Neagu and Georgescu, 2014). In level II, the M/M/s queuing theory model determines the number of charging terminals installed in a CS. Once the number of load terminals is known, the transformer that will serve the CS is sized. Once the transformer sizing in kVA is known, the electrical network is simulated with CymDist software to validate its operability, considering georeferenced scenarios. Considering georeferenced scenarios for the simulation helps determine the conductors' absolute length; with this, the technical losses in the conductors and voltage drops are accurately obtained. The contributions of this article are as follows (Konara et al., 2023).

- A theoretical model for creating fast-charging station infrastructures is introduced based on accessible data obtained from OpenStreetMap. In addition, the proposal is validated using CymDist software for the construction and operational simulation of the fast-charging infrastructure.
- The algorithm is designed to predict the number of EVs and minimize the trajectory of the vehicular flow by employing a traffic rerouting system, considering the topology of the road network.

- The organization and management of vehicular traffic are solved with the Hungarian algorithm and the multiple-product problem; a scalable model is proposed considering hourly mobility patterns.
- The proposed academic model has industrial application potential for charging station infrastructure providers in developing countries.

After this, this article is organized as follows: Section 2 briefly reviews related articles. Section 3 offers the traditional formulation of the problem and the methodology to solve it. Section 4 contains the analysis of the results and the validation of the proposed model with the study of 2 cases. Finally, Section 5 presents the conclusions of this article.

2. Related works

This article studies the characteristics of vehicular flow in a georeferenced area. It will help us dimension and allocate the resources necessary for the correct operation of the EVCSI. A two-level trajectory approach is presented, considering the high stochasticity implied by heterogeneous vehicular traffic. This paper is closely related to three lines of research: vehicular flow analysis in heterogeneous scenarios, allocation of the number of charging terminals for each CS, and optimization of EVCSI required in electric mobility. This section summarizes some of the most current and relevant works related to the proposed study.

2.1. Assignment and location problem

The location of energy supply centers for EVs has been developed in Tang et al. (2018), Chung et al. (2018) considering

Table 1
Category L7e-C EV characteristics.

Vehicle electric	Autonomy (km)	Voltage terminal (V)	Engine (kW)	Maximum speed (km/h)	System regenerative	Vehicle category dimensions (m)
Tazzari Zero	200	230	15–25	90	✓	
Renault Twizy	100	230	17	80	✓	height < 2.5
Audi Urban	73	230–400	15	100	–	width < 1.5
Peugeot BB1	120	230	15	60	–	length < 3.7

Table 2
Types of charging terminals for EVCSI (Campaña and Inga, 2019a).

Type	Current (Amp) Type	Time (h)	Recharge (%)	Power kW	Owner	INEC Standard
Slow	16 AC	8	100	4–8	Public–Private	
Semi-fast	32 AC	1.150	50–80	22	Public	
Fast	63 AC	0.500	50–80	50	Public	61851
Ultra-fast	250–400 DC	0.170	50–80	350	Public	
Change-Battery	AC–DC	0.033	100	–	Public	

the routing problem and EV autonomy as decision variables. Table 1 briefly outlines the characteristics of vehicles designed for urban use in the L7e-C category, where the average travel length of 123 km is observed. The decision problem determines the optimal number of CS, locations, allocation of users to each CS, and economic dispatching policy. In Bi and Tang (2019), the problem is extended to a dynamic planning model by considering the itineraries due to EV usage. Recently, in Napoli et al. (2020), the location problem has been studied by analyzing supply and demand, including the driver's psychological component. In Luo et al. (2020), Balakrishna et al. (2014), in addition to deploying CS, the integration of distributed generation sources are suggested.

The authors have shown that integrating distributed generation helps relieve unplanned loads on existing distribution power grids, which have generally been operating in cities for several years. However, a rigorous analysis that considers road network capacity and vehicle density analysis regarding the topology of the road network defining traffic in cities could not be demonstrated (see Table 2).

2.2. Resource allocation under optimal criteria

Both exact and approximate solution techniques have been applied to solve the resource allocation problem. Accurate solutions involve integer linear programming problems, whereas approximate solutions involve the development of heuristics and metaheuristics (Campaña and Inga, 2019b). Table 3 provides the taxonomy of related studies with a summary of the problem statement, objective function, main constraints, solution methods, and other key features to address the vehicular traffic problem, CS assignment, and sizing.

Recent developments have focused on solving planning problems based on a convex multi-objective model. The model depends on the number of variables and constraints in the optimization problem. Among the issues that have not been adequately considered are those characteristics that bring the problem closer to real-world situations, such as the heterogeneity of the vehicle fleet, vehicle flow routing, road network capacity, and the multiple CS options that the user can resort to recharge the EV batteries and be able to continue with his route.

2.3. Planning of charging infrastructure for EV

The advancement of technology and the constant effort to introduce new concepts of electric mobility on a large scale have encouraged the scientific community to develop products to reduce the CO₂ emissions of conventional private and public transport. Today there are multiple electric mobility alternatives,

such as bicycles, cars, and public transport buses. However, it has not been possible to massively introduce EVs into the land transportation system due to variables that do not make large-scale purchases attractive to potential users in urban and rural areas. These unattractive variables for consumers could be limited autonomy, long charging times, battery life, high costs, and lack of EV charging infrastructure.

In Zhang et al. (2019), the problem is proposed to be addressed by modeling mixed vehicle traffic with different charging terminals and observing EV driving autonomy constraints; furthermore, the mathematical formulation and solution are addressed by linear programming. In Vaziri et al. (2019), Lu et al. (2019), B et al. (2018), Du et al. (2018), Moradipari and Alizadeh (2018), the CS allocation and deployment problem is addressed by partially considering several aspects that guide obtaining robust results; these aspects are: capacity constrained, trajectory probability, travel time, flow conservation, charging time, spatial, temporal collaboration, terminal type, and traffic events. Planning, CS deployment, and setting terminal type selection are essential because EVs present technical constraints such as driving travel range and limited payload. Terminals have been classified according to the charging current the EV can support. The table below briefly describes the different types of existing terminals and their diverse public and private applications (Amry et al., 2022).

As the charging current increases, the time to recharge an EV battery decreases, and the types of charging terminals are different technology. Types I and II are applied in residential areas, and type III is exclusively a public/private service. Type III terminals can reach power ratings of 50–350 kW. Consequently, this article is essential. It covers the EV charging infrastructure planning problem in its integral form, passing through an analysis of vehicular flow, modeling of high stochasticity, projection of vehicle fleet increase with annual rates, and solution of the traffic allocation (Singh et al., 2023; Antarasee et al., 2023). Additionally, routing problems and electrical equipment sizing by observing charging models considering electrical simulation of charging infrastructure in geolocalized areas. Recall that, to size the CS; it is necessary to model the vehicular traffic in trajectory according to the user's need for battery recharging. Therefore, EVCSI must be considered an essential factor during the planning process. In addition, correct planning will allow determining whether or not the different existing electric grids can assume new loads due to the massive introduction of EVs. The main objective is to guarantee the electric service's quality, continuity, and safety. In Campaña et al. (2017), Inga et al. (2017, 2019), a method of cauterization and construction of minimum spanning trees is proposed as an indispensable tool in electrical equipment's optimization and planning processes (Chen and Chen, 2023; Kłos and Sierpiński, 2023).

Table 3
Taxonomy of related studies.

Author, year	Model		Problem			Constraints	Solution			Trajectories		Others
	Theoretical	Experimental	Location Allocation	Route	Obj. function		Exact	Heuristic	Meta-heuristic	Density Traffic	Urban study	
Gan et al. (2020)	✓	-	✓	✓	Maximize Profit Service	Distance Standby time Power grid capacity	-	✓	-	-	-	Elastic demand Stochastic Newton-Raphson NLP
Esteban et al. (2019)	✓	-	✓	✓	Minimize Costs Flows	Capacity Distance	-	✓	-	-	✓	Scalable multi-commodity capacities network
Demir et al. (2019)	-	✓	-	✓	Minimize Travel distance Costs	Flows # Vehicles	-	-	✓	-	-	Deterministic ILP Demand fluctuation NP-hard
Azadi Moghaddam Arani et al. (2019)	✓	-	-	✓	Maximize User Routes Service	Capacity Operation Schedule	✓	-	-	✓	-	Multiple commodity flows network Heterogeneous traffic MILP Branch and Bound Algorithm
Bevrani et al. (2019)	✓	-	-	✓	Minimize Flow Routes	Congestion Expansion tree Conservation flow	✓	-	-	-	✓	Multi-commodity network flow Flow reduction functions NLP Multiple nodes
Campaña and Inga (2019a)	✓	-	✓	✓	Minimize #Charging stations Trajectory Costs	Distance Minimal tree Coverage	-	✓	-	✓	✓	ILP Graph theory Homogeneous nodes
Liu et al. (2019a)	✓	-	-	✓	Minimize Power losses in distribution Maximize Flow	Capacity Congestion	✓	-	-	✓	-	Heterogeneous nodes Optimal Solution Charging congestion during fuzzy multi-objective model
Ghasemi et al. (2019)	✓	-	✓	✓	Min. Transportation cost Minimize shortages Max. humanitarian	Demand Heterogeneous flow Capacity Distance	✓	✓	✓	✓	-	Probability approach Planning periods Multiple-objective PSO Stochastic demand
Campaña and Inga (2019c)	✓	-	✓	✓	Min. Trajectories Min. Charge station Min. Congestion road	Coverage Distance Capacity	-	✓	-	✓	✓	Segmentation ILP Need for Users Neighborhood analysis
Current study	✓	-	✓	✓	Min. Trajectories Min. flow Min. Charge stations Max. Humanitarian	Capacity Distance Coverage Demand	✓	✓	✓	✓	✓	Revised-Simplex MILP Multi-commodity network flow Heterogeneous nodes Scalable Multi-objective NP-Hard Non convex

3. Optimization problem description

This section describes the problem through stochastic analysis of vehicular trajectory traffic and resource allocation for EVCSI. In addition, this section presents the proposed strategy and methodology, followed by the formal problem statement.

3.1. Stochastic analysis of vehicular traffic and resource allocation at EVCSI

EV refueling stations in the public-private transport sector are essential because they supply the primary energy to provide autonomy to the non-conventional vehicle fleet. It is necessary to plan for the massive introduction of EVs in daily traffic, which implies having heterogeneous vehicle networks where the main actors are conventional vehicles and public and private sector EVs.

Most of the research focuses on users and travel time reduction by reorganizing vehicle traffic according to road capacity and considering heterogeneous traffic networks. A fundamental detail is that the demand for vehicle charging is not centered on the nodes (electric or conventional vehicles) but on the flow of the vehicular traffic network.

Therefore, the vehicular traffic flow can simulate the demand generated by EVs exposed in a heterogeneous road network. Consequently, the research aims to solve the problem of resource allocation, traffic routing, and sizing of electric equipment for CS, considering the heterogeneous density of vehicles and their high stochasticity.

We assume that installing a service center for EV battery charging cannot meet the generated demand due to the limited capacity of the CS on a stretch of road. This limitation will cause critical traffic flow due to high coincidence factors for the battery recharge requirement. Consequently, battery capacity is essential for CS deployment and resource allocation. Therefore, we will obtain the following considerations: (i) if there is a CS between a start point and an endpoint of a path, the EV autonomy should be greater than the path length, and (ii) if there is only one CS on the path, the EV autonomy should be more than twice the path length.

An important detail stated so far is that the algorithm knows the multiple paths EV can take regarding Spatio-temporal constraints (distance, path, and flow variability). Furthermore, we consider that the maximum demand for battery recharging in a given area will be provided by the maximum density of vehicles circulating in a given time interval, which can be hourly. This maximum demand or traffic density occurs when the distance between cars and their travel speed is the minimum.

Based on microscopic models for the analysis of vehicle density, we study the maximum admissible density in a georeferenced area considering the variables of spacing between vehicles and the speed at which they travel on the road network. Using a random vector, under Poisson distribution, we generate the variables of speed entry, vehicle spacing, and lengths of the vehicles participating in the road network.

Recall that we can identify whether it is a minibus, bus, or light vehicle by their physical lengths, i.e., by introducing a random vector with sizes of the different types of cars, we can consider the diversity of vehicles that are part of the road network. Consequently, the heterogeneity of cars participating in the road network is evaluated to determine the maximum vehicle density in a time interval and thus allocate resources and dimensions to the EVCSI electrical equipment.

The proposed model for resource allocation and sizing electric vehicle charging centers is a significant breakthrough in charging infrastructure optimization. Using a mixed integer linear programming structure and the column generation algorithm, the

proposed model can solve the complex combinatorial problem of allocating resources for electric vehicle charging in real time, considering traffic flow constraints. The methodology proposed in this model also considers the strategic location of charging centers in places such as shopping malls, parks, and parking lots, which ensures comprehensive and efficient coverage of the charging infrastructure. In addition, using Dijkstra's algorithm to find the shortest route for vehicles based on traffic density, along with simulation in MATLAB and CymDist, ensures the effectiveness of the proposed model.

The model proposed in this study is relevant for scientific research and industrial application in electric vehicle charging infrastructure. The methodology presented in this model has a quantitative approach to allocating resources and minimizing economic and social impacts. The model is highly flexible and can be adapted to different scenarios and locations. The results obtained from the simulation are based on geo-referenced data from a free and public database, which increases the reproducibility and transparency of the study. In summary, the proposed model can potentially be a valuable resource for EV charging infrastructure providers and urban planners in building efficient and sustainable charging infrastructure.

CS deployment planning can consider the optimal location of different charging infrastructures and their influence on power quality, operational safety, and the economics of system operation. Consequently, it is defined as a typical multi-objective optimization problem. This paper will solve the planning problem by considering a multilevel: (i) traffic network and (ii) power distribution network. These categories may overlap, which means that two nodes of each type may be located in the same area. Therefore, at level 1, the traffic network will characterize the flow of vehicles. Finally, at level 2, the capacity in each CS will be studied, considering the number of EVs to be served.

3.2. Proposed strategy and methodology

This paper proposes a theoretical model for resource allocation and sizing of CS with traffic flow constraints in real heterogeneous scenarios. The main objective is to optimize the resources of the loading infrastructure. A non-convex combinatorial problem is proposed under a mixed-integer linear programming structure. Accordingly, the column generation algorithm solves the multi-product flow problem frequently used in MILP.

The column generation algorithm divides the problem into two stages (i) restricted master problem (RMP) and (ii) subproblem. By solving the RMP with the minimum number of variables, we obtain the dual costs for each constrained master problem. This solution is used in the objective function of the subproblem and solved. If the aim of the subproblem value is a negative reduced cost variable, it is added to RMP and cracked again. This process is iterative, and the stopping criterion occurs when the objective value of the subproblem is greater than or equal to zero. When this happens, the constrained master problem can be considered optimal.

In the first level, it is assumed that the driver will choose the shortest path from the starting point (current location) to the destination (CS location) by observing the distance and traffic flow constraints on each stretch of road. In addition, strategic places such as shopping malls, parks, parking lots, customer service centers, and conventional charging stations are considered for CS placement.

At the second level, the CS capacity must meet the hourly demand for EV charging, determined by the type of terminal or technology used for charging. Previous paragraphs mentioned that the kind of charging depends on the batteries' current capacity. Also, the higher the present, the shorter the time it takes to

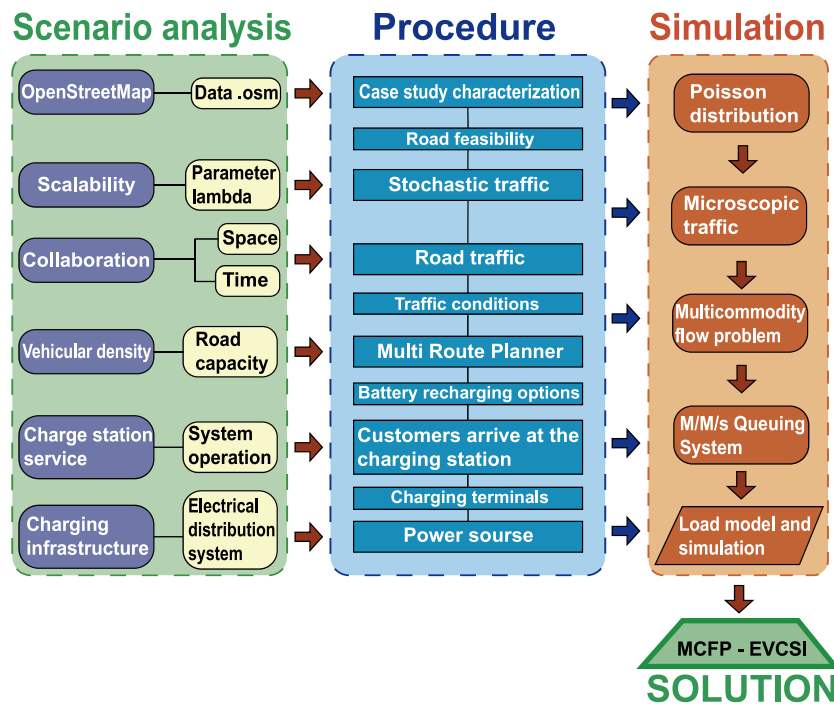


Fig. 2. Methodological flowchart for the construction of MCFP-EVCSI.

charge 20% to 80% of the total capacity of the car battery. Different CS locations and accommodations will cause other impacts on the electrical distribution network. Additional detail is that the Dijkstra algorithm is used to find the shortest path among the multiple routes enabled to generate vehicle network routing based on vehicle density.

Fig. 2 shows the methodology for solving the resource allocation problem and sizing EV charging infrastructure. Four main study groups are proposed to guide the methodological development of this article: (i) scenario analysis, (ii) process, (iii) simulation, and (iv) solution. In the analysis of scenarios, the topology information of the road network of the study area is extracted. In addition, different CS locations in a study area are known, and the nodes where the demand is generated to recharge automobile batteries. Fig. 2 reveals that the georeferenced data are extracted from a free database published in *OpenStreetMap*.

Once the scenario is characterized, the experimental procedure defined by the process and simulation detailed in Fig. 2 is carried out. This process explains the actions, considerations, and variables in the simulation. MATLAB and CymDist software is used for the simulation. After the iterative process, the proposed heuristic returns the maximum vehicle density in the road network during an hourly time interval. This data determines the optimal number of loading terminals required in the road network. Finally, this article is considered basic research because of its experimental nature by applying high-potential simulation processes for EV charging infrastructure providers' industrial applications. It has a quantitative approach to determining resource allocation and minimizing economic and social impacts. This model has an exploratory character, so it is essential to analyze different case studies.

3.3. Problem formulation

This section presents some considerations and a formal description of the problem statement. The multiple product flow problem considers two necessary constraints: (i) travel demand, which means that all products or EVs must be transported to

their destinations or CS, and (ii) the capacity of each intersection of each road segment; this means that the traffic flow at each intersection does not have to exceed its capacity. Therefore, the multi-product flow problem combines several single-product issues, given the limited road capacity and the diversification of heterogeneous vehicle density.

Moreover, the interaction between EVs denotes multiple complexities to solve the single-product flow problem independently. Consequently, the demand generated by each EV is related to various supply options for this demand, and its origin–destination node pair, which refers to the position of EV and CS, can identify it. The CS located in the study area provides the battery recharge supply.

In addition, we assume that the available route based on traffic flow and path capacity can acquire the supply of commodities to meet the demand generated by EVs. The optimal supply to the CS is selected based on the optimal number of charging terminals by observing Spatiotemporal collaboration, which involves minimum displacements with traffic flow constraints on the transport network.

Let us consider $G(\varphi, \mathcal{V}, \mathcal{A})$ a directed graph where φ corresponds to the variable cost of vehicular traffic from an EV to a CS; the distance calculation is performed with the equation *haversine* and is given in km. The set of vertices \mathcal{V} represents the multiple nodes located in the study area as electric vehicles (V_e), charging stations (ε), and intersections (ζ), therefore, $V_e, \varepsilon, \zeta \in \mathcal{V}$ the displacement is given between two source–destination nodes $V_{e_{u,v}}, \varepsilon_{u,v}, \zeta_{u,v} \in \mathcal{V}$ and the set of edges u, v in \mathcal{A} represent the origin and destination respectively.

\mathcal{A} relates the multiple nodes existing in G resulting in the creation of spanning trees at each level. Each track section (ι) has a given number of vehicles (α). Each stretch of road is limited in its traffic capacity (ϖ) and is formed between two vertices at a set of intersections (β). The traffic demand or cumulative cost (W_β) is reflected in each β . The available routes ($S_{1,2,3,\dots}$), where $S \in \mathcal{V}$, are formed from a set of intermediate nodes β , which, dimension the total vehicular flow f_{beta} by assigning a weight W_β on each path.

A section of track can be unidirectional or bidirectional $\beta_{i,j} \neq \beta_{j,i}$. In other words, $\beta \cup \mathcal{S} \in \mathcal{V}$. Let us consider that $\kappa \subseteq \mathcal{V}$ is a subset of sites selected to locate CS where $\kappa \notin \beta$, V_e because the sites selected to locate CS are assumed to be parks, shopping malls, public parking lots.

In addition, $u = \{i \in \mathcal{V} : \exists \beta \in \mathcal{S} | i = 1, 2, 3 \dots m\}$ denotes the subset of the origin nodes in a trajectory and $v = \{j \in \mathcal{V} : \exists \beta \in \mathcal{S} | j = 1, 2, 3 \dots m\}$ denotes the subset of destination nodes, where, m is the size of the vector $\{V_e \cup \varepsilon \cup \zeta \cup \beta\}$.

In other words, the different trajectories (products) are constructed only from the β routes, which are associated with ζ vertices, where the maximum vehicle density generated in β is reflected. This is possible, since, $\sum_{i=1}^m \sum_{j=1}^m \beta_{i,j}, \forall (i \neq j), \in \mathbb{Z}^+$.

Finally, let us consider δ_κ the cost, in terms of vehicle density seen by a CS located in the road network ξ_j where $j \in \kappa$ and n is the maximum number (capacity) of vehicles participating in a longitudinal section of road (ψ) of each CS.

Consider $\mathcal{M} \subseteq \mathcal{A}$ subsets of assigned edges defining the paths enabled in the road network. Therefore, it is $\mathcal{M} = \beta_{i,j}$, $\beta_i \in u$ and $j \in \kappa$. We consider $\mathcal{L} \subseteq \mathcal{A}$ to be a subset of edges of a path \mathcal{L}_i , \mathcal{L}_j where $i, j \in \{\kappa \cup \beta\}$ with this we guarantee that there are no arcs from other families. Next, we define the set of binary resource selection variables.

- ϕ_j allocation variable ε , is 1 when it is found any node that is part of the set $j, j \in \kappa$, 0 in any other way.
- θ_k subset of assigned arcs, if the arc $k \in \mathcal{M}$ it is used, otherwise 0.
- τ_e^j path enabled, is 1 if the edge $e \in \mathcal{L}$ and $j \in \kappa$, otherwise 0.

$$f_{\beta(m)} = \sum_{m=1}^s W_{\beta(m)} \left(\frac{\text{veh}}{km} \right) \quad (1)$$

$$W_{\beta(m,n)} = \sum_{m=1}^{V_e} \sum_{n=1}^{np} \frac{q_{(n)}}{S_{p(m)}} \left(\frac{\text{veh}}{km} \right) \quad (2)$$

$$q_{(m)} = \sum_{m=1}^{np} \frac{\alpha_{(m)}}{t_s} \left(\frac{\text{veh}}{hra} \right) \quad (3)$$

$$\alpha_{(m)} = \sum_{m=1}^{np} \varpi_{(m-1)} * \Theta \quad (\text{veh}) \quad (4)$$

$$\varpi = \sum_{m=1}^{np} \sum_{n=1}^A \frac{\iota_{(n)} + s_{(n)}}{np} \quad (\text{veh}) \quad (5)$$

Eqs. (1) and (2) are used to calculating the total and partial concentration of vehicles in a specific length. Eq. (3) expresses a vehicle flow on a stretch of the road network that corresponds to the frequency with which a given number of vehicles pass in a specific time. Eq. (4) calculates the average number of cars in a lane as a function of the length of the road cross-section and the spacing between vehicles. Theta is an annual rate of increase in the vehicle fleet.

It is assumed that the spacing between vehicles is uniform and that the maximum capacity of a road cross-section occurs at the minimum distance between vehicles and the minimum speed. Finally, the equation (5) is used to calculate the number of cars as a cross-section length and spacing function. It is essential to mention that a microscopic model has been used for the analysis of traffic flow, which considers ι , S_p , and s . Therefore, the multi-product transportation problem can be formulated as follows:

Objective function:

$$\text{Min: } Z_{(q)} = \sum_{k=1}^t q_k \theta_k \quad (6)$$

Subject to:

$$\sum_{k=1}^t \theta_k^i = 1, \quad i = 1, 2, \dots, u(k) \quad (7)$$

$$\sum_{k=1}^t \theta_k^j = 1, \quad j = 1, 2, \dots, v(k) \quad (8)$$

$$\sum_{k=1}^t \theta_k^i = f_{\beta}|_k^i, \quad i = 1, 2, \dots, u(k) \quad (9)$$

$$\sum_{k=1}^t \theta_k^j = f_{\beta}|_k^j, \quad j = 1, 2, \dots, v(k) \quad (10)$$

$$\sum_{k=1}^t \theta_k = \varphi \quad (11)$$

$$\sum_{k \in S} \theta_k \leq |S| - r(S), \quad \forall S \subseteq \mathcal{V}, S \neq 0 \quad (12)$$

$$\theta_k, \quad \in \{0, 1\} \quad (13)$$

Eq. (6) corresponds to the objective function. Eqs. (7) and (8) ensure that vehicular flow is directed from the service nodes to the demand nodes. Eq. (9), (10), and (11) correspond to the vehicular concentration restrictions for the corresponding route, observing capacity criteria in each road section. Eq. (12) guarantees the search for the dual variables and their aggregation. Finally, equation (13) declares the binary variable. Furthermore, $q_k = [q_1, q_2, \dots, q_m]^T$ where $k = 1, 2, \dots, t$ and represents the vehicle density of each commodity. The cumulative capacity of the EV is represented by $f_{\beta} = [W_{\beta 1}, W_{\beta 2}, W_{\beta \dots m}]^T$, and $\varphi = [\varphi_1, \varphi_2, \dots, \varphi_{\dots m}]^T$ respectively. The adjacency matrix between vertices and edges is represented by $\mathbf{G} = [G_{ij}]_{m \times m}$. The length of $m \times m$ is a function of the total number of vertices in the scenario. Finally, $f_{\beta}|_k^i = [f_{\beta}|_k^1, f_{\beta}|_k^2, \dots, f_{\beta}|_k^m]$, and $f_{\beta}|_k^j = [f_{\beta}|_k^1, f_{\beta}|_k^2, \dots, f_{\beta}|_k^m]$ con $k = 1, 2, \dots, t$ is defined as follows.

$$f_{\beta}|_k^i = \begin{cases} -W_{\beta}|_k^i & \text{si } i = u(k) \\ W_{\beta}|_k^i & \text{si } i = v(k) \\ 0 & \text{any other case} \end{cases} \quad (14)$$

$$f_{\beta}|_k^j = \begin{cases} -W_{\beta}|_k^j & \text{si } j = u(k) \\ W_{\beta}|_k^j & \text{si } j = v(k) \\ 0 & \text{any other case} \end{cases} \quad (15)$$

3.3.1. Column generator

In this article, we are going to use the column generation method. This method allows us to solve extensive linear programs. To do so, we consider the following assumptions: (i) the variables are non-basic, (ii) the variables will assume a value greater than or equal to zero in the optimal solution, (iii) an initial subset of variables must be considered to solve an initial problem and (iv) the problem can be divided into a primal and dual problem. The idea is to take advantage to generate variables that have the potential to improve the objective function. The process of the algorithm is as follows.

The primal problem is solved with a subset of variables considered; with this solution, we obtain the dual costs for each constraint of the primal problem. We assume that χ_*^k is the optimal value of the dual objective function that was solved by

the revised simplex method; if the value of the dual objective is a negative reduced cost such that $\chi_*^k < 0, \forall k = 1, 2, \dots, t$ this variable is added as a column to the primary problem and the problem is resolved iteratively.

When $\chi_*^k \geq 0, \forall k = k_1, k_2, \dots, k_p$, the algorithm stops, and we can conclude that the primal problem is optimal. For each linear problem, there is a problem that is solved in parallel. The latter is known as the dual problem. We consider the following issue to solve the primal and dual problems.

$$z = cx, \quad (16)$$

Subject to:

$$Ax \leq b \quad (17)$$

$$x \geq 0 \quad (18)$$

The linear problem of Eqs. (16) and (17) obtains a dual counterpart.

$$z = c\omega, \quad (19)$$

$$A\omega \leq b \quad (20)$$

$$\omega \geq 0 \quad (21)$$

Eqs. (19)–(21) have the same terms, except for the time $\omega = C_{BV}B^{-1}$, which is a variable that is assigned to the equation (17) of the first formulation, where $\omega = C_{BV}B^{-1}$, which corresponds to an iteration of the revised simplex method and is known as a dual variable array. The variables $C_{BV}B^{-1}$ and B^{-1} correspond to the coefficients of the essential variables and the connectivity matrix relating vertices and edges, respectively. Consequently, the problem illustrated in Eq. (6)–(12) can be separated into two primary and secondary issues, respectively. The equations defining each primary and secondary problem are presented as follows.

Primal–Primary Problem

Objective function:

$$\text{Min: } z_{(q)} = \sum_{p \in \beta} \sum_{k=1}^t q_k \Psi_p \theta_{pk} \quad (22)$$

Subject to:

$$\sum_{p \in \beta} \Psi_p \sum_{k=1}^t \theta_{pk} = f_\beta |_k^i, \quad i = 1, 2, \dots, u_{(k)} \quad (23)$$

$$\sum_{p \in \beta} \Psi_p \sum_{k=1}^t \theta_{pk} = f_\beta |_k^j, \quad j = 1, 2, \dots, v_{(k)} \quad (24)$$

$$\sum_{p \in \beta} \Psi_p \sum_{k=1}^t \theta_{pk} = \varphi \quad (25)$$

$$\sum_{p \in \beta} \Psi_p = 1 \quad (26)$$

The new set β is used in each iteration to identify the generated routes, and Ψ is a partial solution to the primal problem. Eq. (22) is the objective function of the primal problem, and Eqs. (23)–(25) are the vehicle concentration and road capacity constraints, respectively, which allow restricting the solution space to routes that only meet a little value. Eq. (26) guarantees a non-zero solution to the secondary problem.

Dual–secondary problem

Objective function:

$$\text{Min: } \chi_*^k = \sum_{k=1}^t q_k \theta_k - \pi_3 \sum_{k=1}^t \theta_k^i - \pi_2 \sum_{k=1}^t \theta_k^j - \pi_1 \sum_{k=1}^t \theta_k - \pi_0 \quad (27)$$

Subject to:

$$\sum_{k=1}^t \theta_k^i = 1 \quad (28)$$

$$\sum_{k=1}^t \theta_k^j = 1 \quad (29)$$

$$\sum_{k \in S} \theta_k \leq |S| - r(S), \quad \forall S \subseteq V, S \neq \emptyset \quad (30)$$

$$\theta_k \in \{0, 1\} \quad (31)$$

Eq. (27) is the objective function of the secondary problem, so χ_*^k is the reduced cost variable, provided that $\chi_*^k \neq 0$ can find dual variables to be inserted in the main problem. Eqs. (28) and (29) are constraints that allow CS and points where demand is generated to search for the best route within the road network. In Eq. (30), the coefficient r is selected from the set S that will allow verifying the cost of the negative reduced variable. Finally, the binary selection variable is declared with equation (31). Fig. 3 shows the flowchart for resource allocation and sizing of electrical equipment required in EVCSI.

3.3.2. Optimal number of load terminals

This section describes the methodology used to determine the optimal number of charging terminals in each service station for recharging batteries in electric mobility. The charging terminals are in charge of providing the recharging service for batteries in electric mobility. Such service is stochastic and conforms to queuing systems, specifically M/M/s systems. M/M/s systems consider multiple service stations and waiting times in the queue before being served by a charging terminal. Consequently, the M/M/s system, applied in queuing theory, describes several customers expected to arrive, followed by a queue generated before being served by an available loading terminal. Once filled, the customer exits the system as illustrated in Fig. 4.

The arrival of EVs to the CS is an independent event and satisfies stationarity conditions, Markov's properties, and universality. Consequently, the appearance of EVs at the CS is given according to the Poisson process, and the time intervals between vehicles assume a negative exponential distribution. For the output system, the charging time for each EV depends on the remaining energy in the battery, so a negative exponential distribution is used to describe the charging time. Another aspect to consider is that the charger can only serve one vehicle at a time and is serviced on a first-come, first-served basis, as illustrated in Fig. 4. On the other hand, the charging station can serve more than one electric vehicle simultaneously because of its M/M/s characteristic for $s > 1$.

The system is affected by the initial state and the time elapsed since the start of a transient condition. After sufficient time has elapsed, the system becomes independent of the initial state, and the time elapsed becomes steady. Another consideration is that the number of customers entering the system must equal the number of customers leaving. Consequently, the probability that satisfies this condition is:

$$P_o = \frac{1}{[\sum_{\eta=0}^{M-1} \frac{1}{\eta!} \left(\frac{\lambda}{\mu}\right)^\eta] + \frac{1}{M!} \left(\frac{\lambda}{\mu}\right)^M \frac{M\mu}{M\mu-\lambda}} \text{ para } M\mu > \lambda \quad (32)$$

$$\lambda = \frac{\eta}{\text{station opening time}} \quad (33)$$

$$\mu = \frac{1}{\text{average load time}} \quad (34)$$

Where M is the number of available charging terminals, λ is the average arrival rate, μ is the average service rate in each

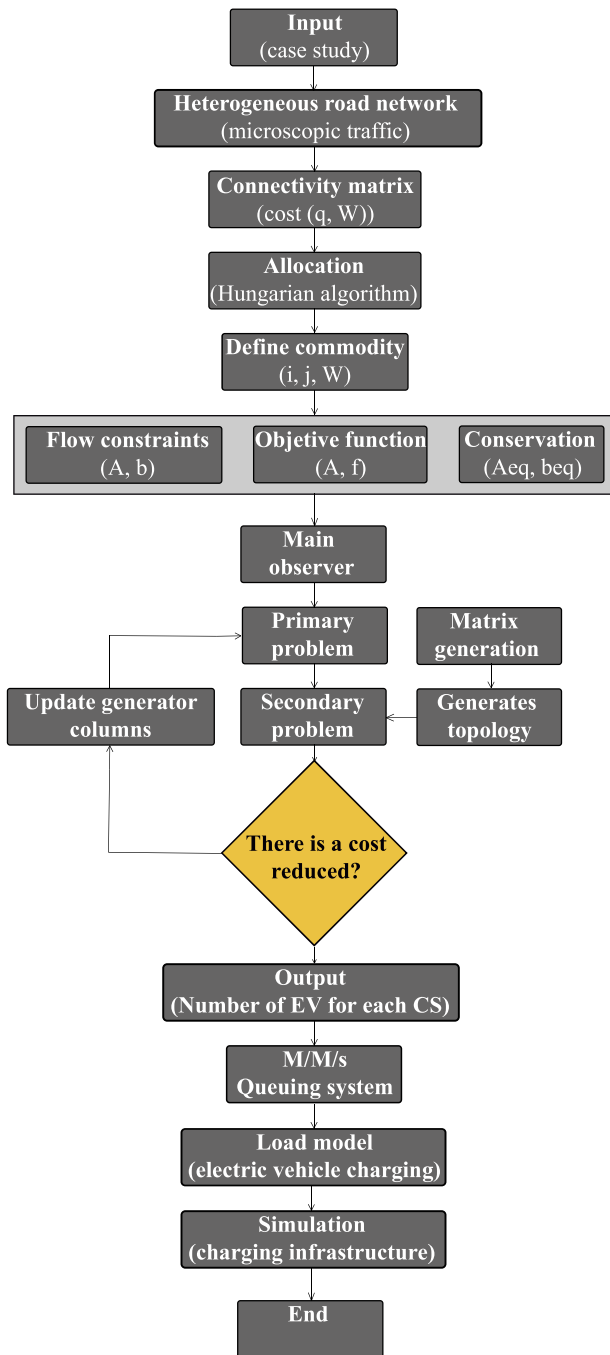


Fig. 3. flowchart for solving the multicommodity flow problem for developing electric vehicle charging station infrastructures. (MCFP-EVCSI).

channel, and η is the number of EV units in the system. Finally, \mathcal{W}_s defines the average time an EV stays in the system.

$$\mathcal{W}_s = \frac{\mu \left(\frac{\lambda}{\mu} \right)^M}{(M-1)!(M\mu-\lambda)^2} P_0 + \frac{1}{\mu} \quad (35)$$

Through \mathcal{W}_s and P_0 curves as a function of the number of terminals M , the optimum number of chargers is selected. Consequently, it is possible to determine the CS topology and the maximum installed power to be foreseen for CS operation. Another detail is that once the installed power and the topology of the charging stations are known, the feeder that will connect to the primary distribution transformers is laid through minimum spanning trees. Therefore, it is possible to guarantee the reduction

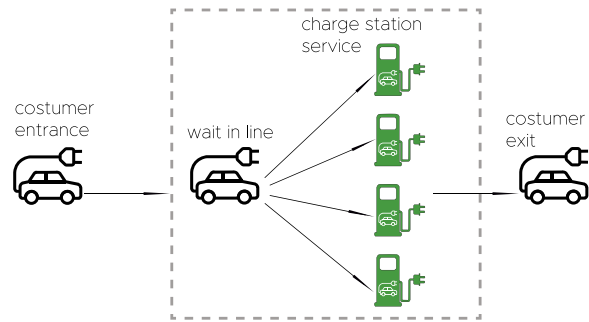


Fig. 4. M/M/s queuing system scheme.

of costs of the feeder; additionally, thus the technical losses that may affect depending on the longitudinal variable of the feeder.

3.3.3. EV charging model

The massive introduction of EVs into the electric current flowing through the conductors of the distribution network. For correct planning of charging infrastructures, it is necessary to guarantee the availability to recharge the batteries of electric vehicles when the EV operator requires it. In this context, the present proposal seeks to determine the maximum power that should be installed in each CS so that the electric supply is guaranteed at the moment required by the non-conventional mobility user. Therefore, it is necessary to mathematically represent the characteristics of the distributed loads. The load model represents the mathematical relationship between the magnitude of voltage and active and reactive power flowing in the feeder. In this paper, the CymDist software is used, which allows simulation of the load under two methodologies (i) exponential and (ii) polynomial. This paper will use the polynomial model to determine the EV loading model. Then, to select the polynomial model, it is necessary to define coefficients and exponents. The exponents specify the load type, such as constant power, constant current, and constant impedance, while the coefficients define the relative proportion of each load type. The active and reactive power expressions described in the polynomial model (ZIP) are represented by Eqs. (36) and (37), respectively.

$$P = P_0 (p_1 \bar{V}^2 + p_2 \bar{V} + p_3) \quad (36)$$

$$Q = Q_0 (q_1 \bar{V}^2 + q_2 \bar{V} + q_3) \quad (37)$$

V_0 , P_0 , Q_0 represent the voltage, active and reactive power when the supply voltage corresponds to 1 p.u in Eqs. (36) and (37), $p_1 - p_3$ and $q_1 - q_3$ are parameters of the models that when approaching 1 imply that the load behaves as a constant impedance, a continuous current consistent or a regular power, respectively. The independent parameter V of (38) is the p.u. Supply voltage. If the actual supply voltage is equal to the voltage V_0 , then V will also be equal to 1, as shown in (38).

$$\bar{V} = \frac{V}{V_0} \quad (38)$$

The coefficients defining the polynomial static model are shown in Table 4 below.

Finally, it is essential to model the load represented by the electric vehicle on the grid, not only because of the increase in current that this means but also because the electric chargers include in their model a harmonic current source based on a three-phase converter with a 12-pulse bridge, which represents the non-linear characteristic due to its power electronic components.

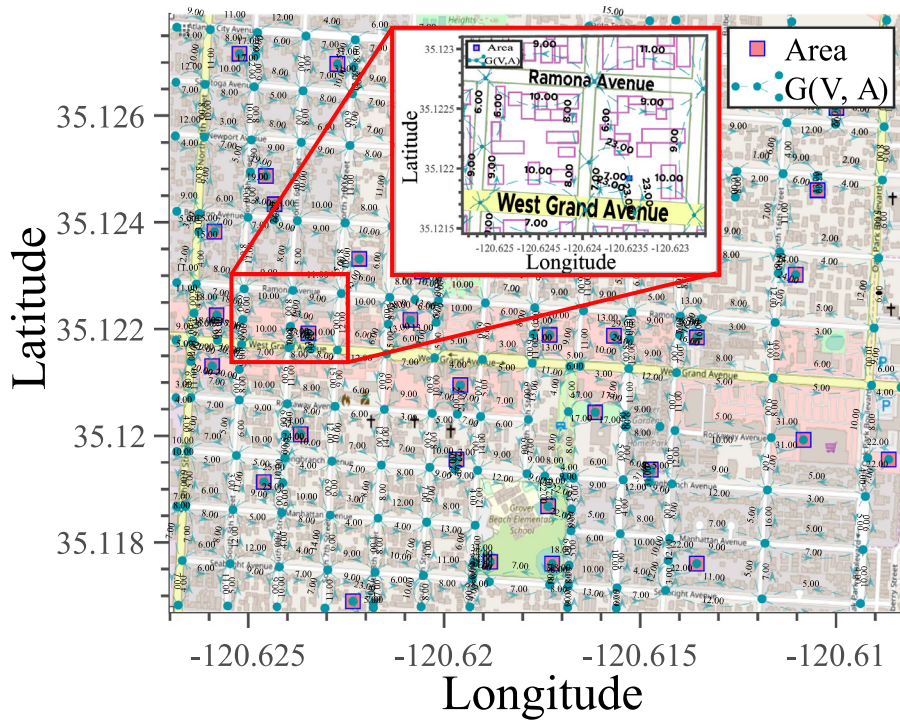


Fig. 5. Case A, Grover Beach with an area of 2.13 km^2 , a city in San Luis Obispo County, US state of California.

Table 4

EV charge static load model parameters for fast charger (480 V) (Tian et al., 2021).

	Coefficient	Parameter
Active power	p_1	-0.1326
	p_2	0.1816
	p_3	0.9495
Reactive power	q_1	-
	q_2	-
	q_3	-

4. Analysis of results

This section presents the results obtained by the MCFP-EVCSI heuristic model for the creation of EVCSI. The microscopic model has been used to simulate the input variables, which allows for studying the relationship between speed, length, and separation between vehicles participating in the road network. Table 5 shows the simulation parameters, where the need to consider the input variables is observed by analyzing heterogeneous and scalable vehicular traffic in georeferenced areas. In addition, as this article is experimental, two case studies are developed to validate the proposed heuristic. In this way, it will be possible to dimension CS for EVs and allocate resources for energy supply in charging infrastructures.

4.1. Case study A

Case study A is illustrated in Fig. 5, and it can find the topology of the road network to be analyzed in this case study. We have important information such as (i) connectivity matrix, the direction of the road, and weights assigned for each section included in the optimization model. Consequently, the longitudinal relationships from an intersection i to a meeting j are known to the model. Considering the actual data in each case study will allow us to approach reliable solutions and, in addition, will let us know the maximum capacity of the road network in each cross-section.

Table 5

Simulation parameters.

Deployment	Density EV	Variable
Allocation	Study cases	A-B
	Study areas	0.99 y 2.13 km^2
	Geographical area	Urban
	Geographic reference	Latitude–Longitude
Application	Annual rate	Variable
	Scalability	4 years
	Spacing	Variable
Traffic	Charging terminal	AC–DC
	Safety distance	3–6 m
	Vehicular flow	Variable
	Vehicular concentration	Variable
	Vehicular speed	[20 40 60] km/h
Deployment	Light	4.3 (m) \leq
	Buses	15 (m)
	Trucks	12 (m)

Fig. 6 presents the variation of vehicle concentration as a function of different incremental rates over 20 years. The maximum number of vehicles circulating in each case study is determined based on the maximum vehicle density. The total rate corresponds to a theoretical value, which the designer of the vehicular network can adjust. Its value will depend on the studies and projections estimated in each zone of its different central administrations.

The randomness of the scenario has been recreated using the discrete Poisson probability, as suggested in the literature. The analysis of the increase in the vehicle fleet has been performed over 20 years with four annual rates Θ as shown in Fig. 6. There is a technically linear trend in the first ten years of analysis, which does not occur after the eleventh year. The slopes cease to be constant as the annual rate of the vehicle fleet increases. Another interesting detail revealed by Fig. 6 is that, as the average speed at which vehicles circulate increases, vehicle density decreases, i.e., they are inversely proportional. In purple (see Fig. 6) represented the empirical values that show the number of values

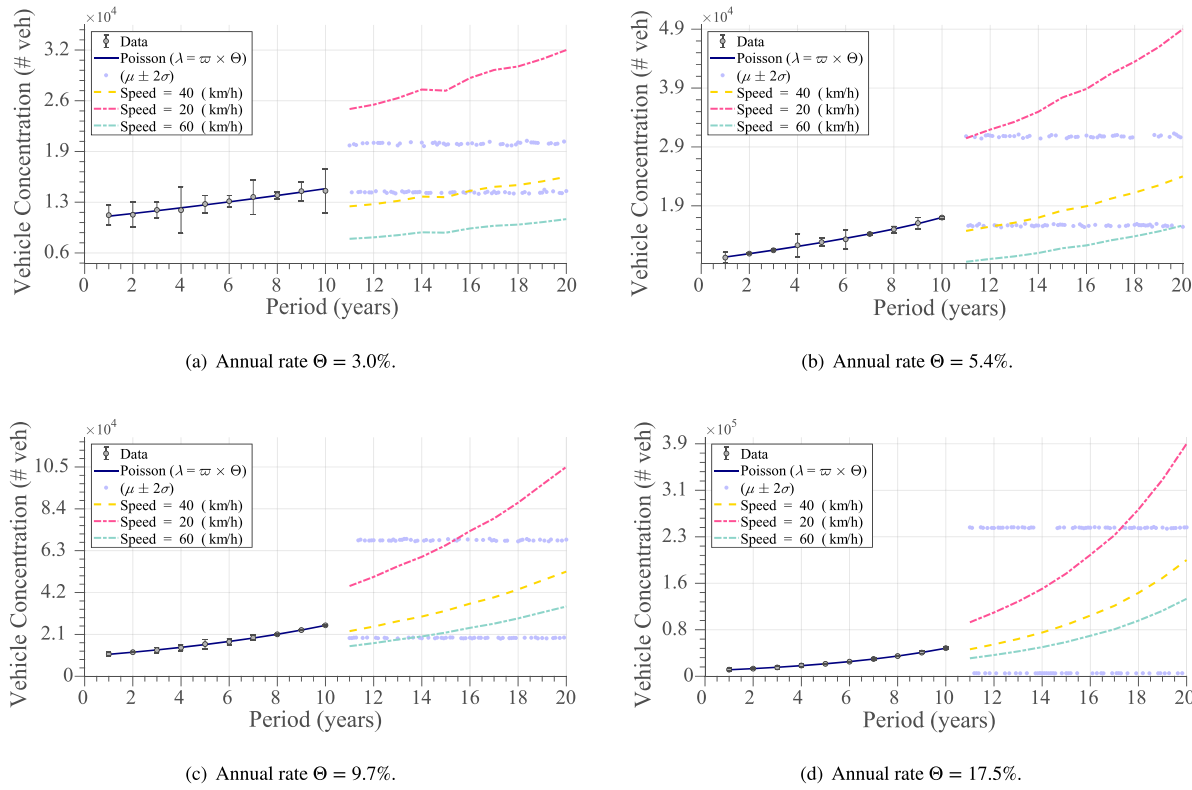


Fig. 6. Case A: Microscopic traffic flow analysis using discrete Poisson probability.

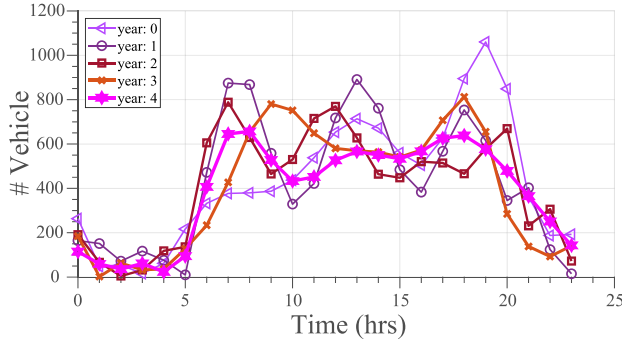


Fig. 7. Vehicular traffic scalability with the incremental rate of 3% for case studies A and B.

above and below the average value of the three analyzed speeds in the 11 to 20 years. It means that approximately 95% of the data are above and below the average. Its importance is visualized in Fig. 6. Therefore, this article considers speed, geometric road layout, spacing, and annual growth rates as fundamental variables to achieve results that satisfy optimal solutions in real scenarios.

Fig. 7 illustrates the number of vehicles distributed over 24 hours for study cases A and B. The trend in Fig. 7 corresponds to the weekly average of vehicular traffic behavior in its standard working day conditions. The model proposed in this article is evaluated over four years from year zero, and an incremental rate of 3% is considered for both case studies. This cumulative rate has been taken as a reference from the literature. Therefore, this variable is adapted to any reality or case study that is specifically required.

The hourly variability of the number of vehicles circulating in a given area responds to a normalized random vector considering the original trend (year zero) and the annual incremental

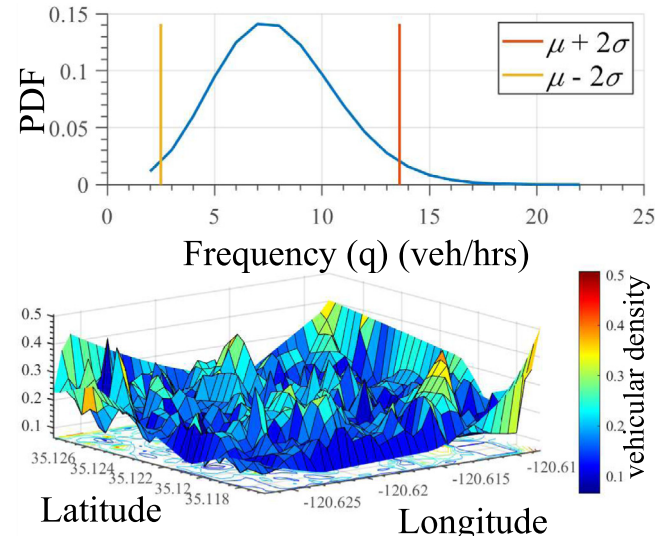


Fig. 8. Vehicle density distribution located in geolocated scenario case A.

rate. In addition, Fig. 7 shows that the highest vehicle density is distributed from 07:00 to 20:00 hours. Consequently, charging stations should be designed to meet the demand during peak traffic hours in a given area.

With Fig. 8, we illustrate, through the frequency graph, the random distribution of vehicle density in an area in trajectories. With the heat graph in Fig. 8, we can appreciate the areas of higher vehicle density represented by the yellow and red vertices.

The adjacency matrix allows us to understand the data distribution within the case study. Fig. 9 shows two techniques for

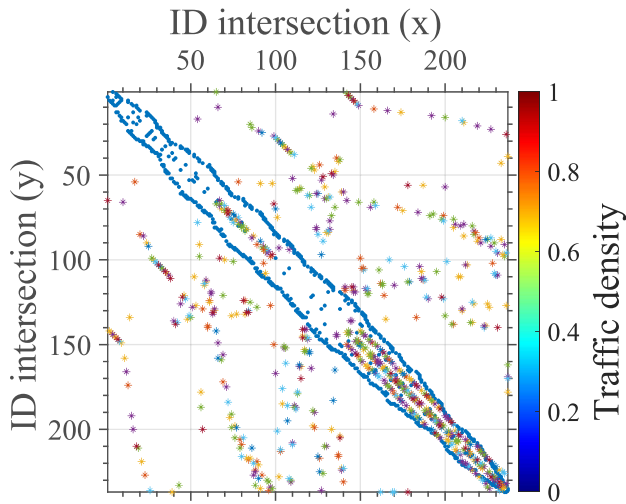


Fig. 9. Case A: Distribution of connectivity matrix and its nodal relationship.

reordering the sparse adjacency matrix: (i) the inverse Cuthill-McKee algorithm and (ii) column permutation. In solid blue color in Fig. 9 illustrates the inverse Cuthill-McKee algorithm, which has a clear tendency to group its non-zero elements closer to the diagonal, preserving at the same time, the special relationship of each edge (i, j) with its nodes $i = j$ and $j = i$. For its part, the column permutation algorithm illustrated in Fig. 9 allows reordering the columns of the sparse-type matrix in non-decreasing order of non-zero count. This metric enables visualizing the different randomly assigned magnitudes of vehicle density that will be considered to evaluate the model proposed in this paper. Therefore, Fig. 9 shows that the input data are stochastic, resulting from a microscopic analysis that allows us to understand vehicular traffic. Thus, we use the tiny model to solve MCFP-EVCSI as a directed graph to model the traffic rate and the maximum vehicle concentration at level 1.

Fig. 10 illustrates the algorithm's performance evaluated in a scalable scenario from year 0 to year 4. Fig. 10(a) shows the machine time to solve the primary problem. It is easily observed that the machine time used to solve the primary problem depends on the time interval in which the analysis is developed; this response to the stochasticity of the vehicular flow in each time interval during working days. Furthermore, with Fig. 10(a), the trend of machine time as a function of the annual growth rate of the vehicle fleet is increasing with a minimum of 3 min in year 0 and a maximum of 4.7 min in year 4.

The linear problem is constructed as the primary concern. Therefore, the machine time is greater than the time spent on the second problem, as illustrated by comparing Fig. 10(a and b). With Fig. 10(c), the observer's machine time is presented, which has the function of deciding on the growth of the column generator, i.e., it is the one that verifies if there is reduced cost in its objective function to add it as a solution. Once a feasible solution has been added, the algorithm repeats the iterations from the primary and secondary problems, and the observer makes decisions based on the negative cost variables.

A curious fact to note with Fig. 10(d) is that the cost of the objective function in each scenario tested maintains the same trend, i.e., there is no deviation of data from year 0 to year 4. The movement in Fig. 10(d) responds to the immutability of the scenario topology. That is, it increases vehicular traffic as a function of time, but the topology of the case study remains the same. Finally, Fig. 10(d) shows that the objective function is inversely proportional to the hourly characteristic curve that

defines the vehicle density in Fig. 7. This inverse behavior is linked to operating costs; this means that the design and sizing of electric vehicle charging stations must function the peak demand from 07:00 to 20:00 hours on ordinary days from Monday to Friday. Therefore, the objective function has a minimum cost in high-demand hours because it manages to justify the sizing of the CS, and the cost of the objective function is maximum where traffic demand is minimum; it is because, in those low-demand hours, the recharging infrastructure is not used, so, somehow there is an over-sizing in low demand hours.

Table 6 shows the resulting metrics for case study A. In each column, respectively, the ID of the charging station, the geographical coordinates in latitude-longitude, the vehicle concentration, and the number of vehicles in the hour of maximum demand can be seen. The charging station with ID 4 should serve a maximum number of 49 cars during the period of maximum vehicle demand. It is essential to remember that the analysis assumes 100 percent EV penetration in the road network. Furthermore, Fig. 7 shows that the maximum demand in year 0 occurs at 19:00 hours with 1151 vehicles distributed in the geographical area. The load distribution of the cars is to be managed by each charging station during the 19:00 hour of year 0. It is presented in Table 6. The distribution of vehicle charging for the rest of the day is given by a percentage pattern that creates the trends in Fig. 7. However, in this case, we have considered the maximum demand for vehicles in a time interval to estimate the maximum electrical power installed in the different CS distributed in the study area.

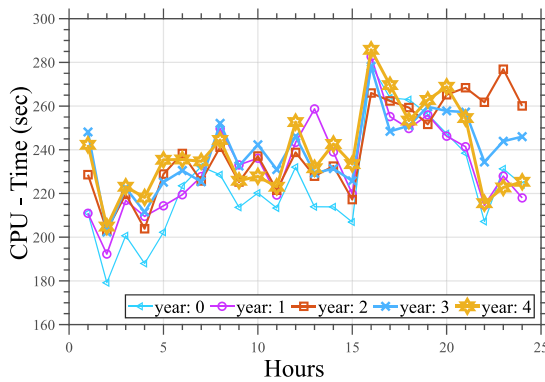
The installed electrical power of a CS should be directly proportional to the number of charging terminals required to meet the demand for EV battery charging. In addition, the number of charging terminals will depend on the technology (50 MW–350 MW) and the number of vehicles requiring the service during periods of high demand. For example, if we consider the time 19:00 in Fig. 7 and look at Table 6 illustrating the distribution of vehicle charging, we observe that the charging station with ID 4 should serve 49 vehicles for 1 hour.

4.2. Case study B

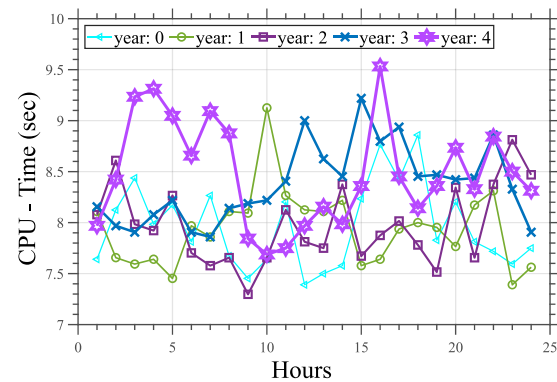
Next, the model's adaptability to a new case study is verified. This case study is in Arroyo Grande County, San Luis Obispo County, California, United States. In addition, they will analyze what happens with the different vehicle flows in each hourly interval with a growth rate of 3.0% and verify contingencies of up to $N - 2$. The contingency refers to the departure from the operation of a CS. The scenarios are simulated in which CS has to go out of the process due to any event. Finally, the effect caused by a vehicular flow that each CS attend is analyzed.

Fig. 11 shows the geographic area in which case study B will be analyzed. There are nine CS for VE identified with labels. An additional detail visualized in dark green is the bi-directionality of each road section and how it relates to each intersection. In addition, Fig. 11 identifies the costs directly associated with the vehicle density on each roadway.

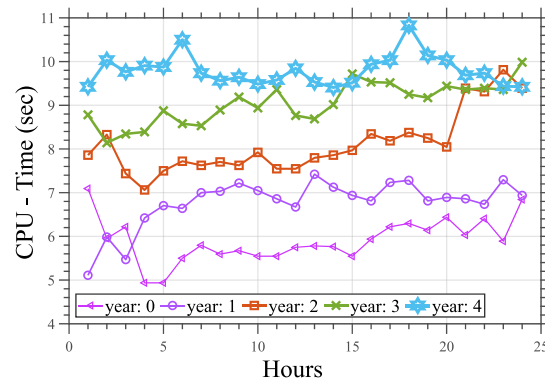
Fig. 12 presents the graphical solution to the transportation problem considering maximum vehicle flow during a time interval. The magnitude of the vehicle density generated at each link is visualized in black. The resulting vehicle density at each node is easily identified in red, the sum of the flows entering each node minus the flows leaving. It is called the conservation of vehicle flow. This condition is critical to maintaining the nodal equilibrium criterion, which satisfies the equations of the mathematical problem statement. The negative red sign indicates the flows to be served by each recharging station; remember that the negative sign indicates that it is a supply node (recharging station). A fundamental condition for the convergence of the model is that



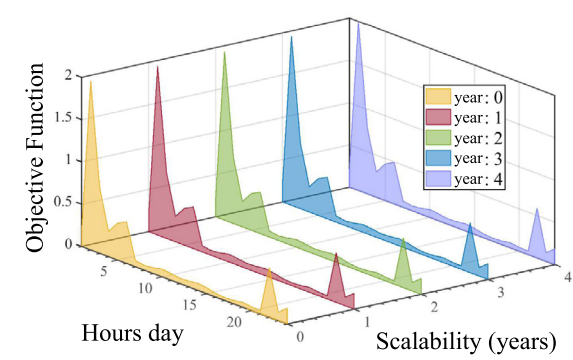
(a) Machine time to solve the primary problem.



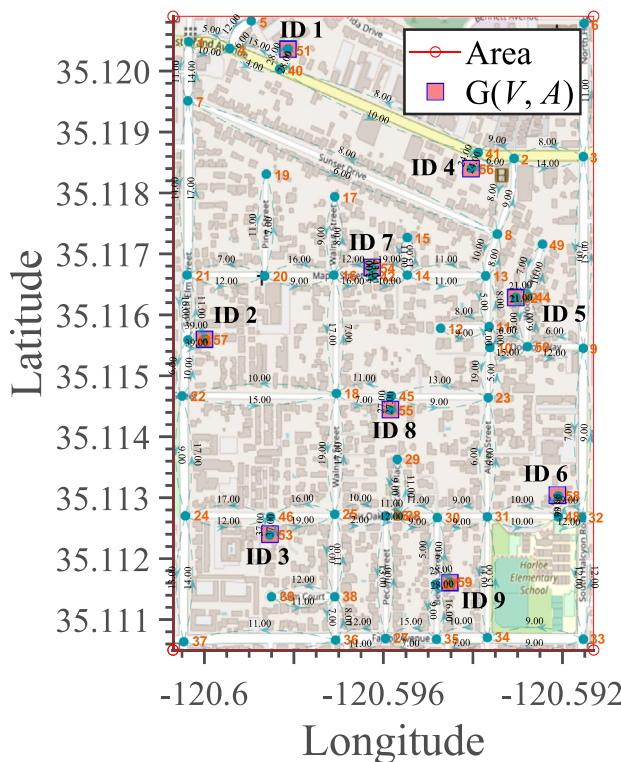
(b) Machine time to solve secondary problem.



(c) Observer machine time.



(d) Cost of the objective function.

Fig. 10. Case A: Performance of the algorithm considering scalability of 4 years with a growth rate of 3%.**Fig. 11.** Case B: Weights assigned on each track section with microscopic analysis in an area of 0.9887 km^2 .

the supply centers with negative signs cover the demand with a positive signal at each intersection.

In the planning algorithms, a fundamental criterion for equipment sizing is considering critical cases of high demand. This consideration will allow us to approach the optimal sizing of the resources required in the planning processes, guaranteeing to cover the market. Consequently, **Table 7** is presented the result of the analysis case in **Fig. 11** where the critical issue is considered. The fundamental problem occurs at the maximum density of vehicles driving in the geolocated area. These extreme conditions occur at minimum travel speeds with minimum car separation distances. Column one of **Table 7** presents the index of charging stations; column two illustrates the resulting concentration of vehicles to be served by each CS. The sign of the second column is negative because the model considers it a node contributing to the transportation system to form the equilibrium equations, where the supply nodes must cover the sum of the partial flows observed at each intersection. Consequently, we denote those consumption nodes, and with the negative sign, we identify the nodes that satisfy the equilibrium equations of the multiple-product problem.

In addition, **Table 7** in the third column shows the number of vehicles each CS will have to serve under critical conditions of high vehicle density without considering contingencies. Finally, the last row of **Table 7** identifies the maximum number of vehicles in an instant of time, which in this case is 348 vehicles, as the maximum admissible density in the area considered for the analysis. Consequently, with the number of cars to be served by each CS and the maximum traffic density in trajectory, we can size and foresee the necessary resources for constructing the recharging infrastructure in the geolocalized areas.

Table 6

Case A: Maximum partial demand in each CS at hour 19:00 with 32.97 km of road network in contingency N - 0 corresponding to year 0.

ID	Longitude	latitude	Concentration Vehicular	Vehicles (#)
1	-120.625225787882	35.1271587155963	-0.77	25
2	-120.622727167999	35.1269678899083	-1.31	43
3	-120.617829873029	35.1267623853211	-0.64	21
4	-120.609994201077	35.1261458715596	-1.48	49
5	-120.615391220024	35.1256174311927	-1.29	42
6	-120.620588349380	35.1256467889908	-1.43	47
7	-120.624546163274	35.1248688073394	-1.09	36
8	-120.624326284724	35.1243403669725	-0.85	28
9	-120.619488956631	35.1240174311927	-1.43	47
10	-120.610473936095	35.1246045871560	-1.44	48
11	-120.611033626948	35.1230192660550	-0.67	22
12	-120.620568360421	35.1230779816514	-0.64	21
13	-120.622167477145	35.1233128440367	-0.85	29
14	-120.625865434572	35.1238266055046	-0.62	20
15	-120.625805467695	35.1222559633028	-0.61	20
16	-120.623466759484	35.1219183486239	-1.18	39
17	-120.620868194807	35.1221678899083	-0.92	30
18	-120.617310160094	35.1218889908257	-0.86	28
19	-120.615671065451	35.1218743119266	-0.99	33
20	-120.613552235790	35.1218449541284	-1.44	47
21	-120.610833737358	35.1199220183486	-1.21	40
22	-120.614731584375	35.1193642201835	-1.34	44
23	-120.616150800468	35.1204357798165	-0.96	32
24	-120.619588901427	35.1209495412844	-0.85	28
25	-120.625925401449	35.1213018348624	-0.97	32
26	-120.623666649075	35.1200247706422	-0.79	26
27	-120.619688846222	35.1195550458716	-0.81	27
28	-120.624606130151	35.1191293577982	-1.37	45
29	-120.617350138012	35.1186743119266	-1.19	39
30	-120.617250193216	35.1176027522936	-0.80	26
31	-120.618829320982	35.1176321100917	-1.09	36
32	-120.622327388818	35.1168981651376	-0.94	31
33	-120.613552235790	35.1176027522936	-0.61	20
34	-120.616050855673	35.1232541284404	-0.87	29
35	-120.608654940820	35.1195550458716	-0.62	20
Total			-34.92	1151

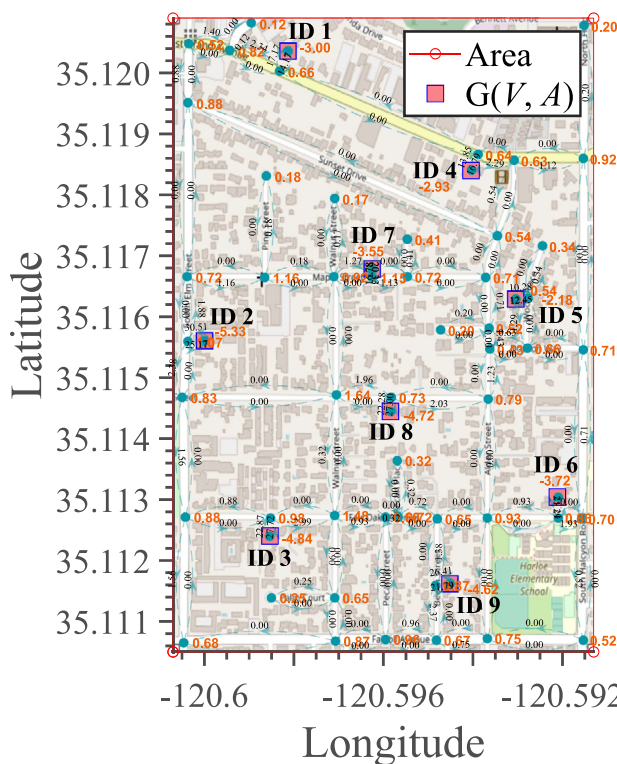


Fig. 12. Case B: Graphical solution to the multiple product problem.

Table 7

Case B: Maximum partial demand in each CS with 9,984 km of road network in contingency N - 0.

ID	Vehicle Concentration	# Vehicles
1	-3.00	30
2	-5.33	53
3	-4.84	48
4	-2.93	29
5	-2.18	22
6	-3.72	37
7	-3.55	35
8	-4.72	47
9	-4.62	46
Total	-34.89	348

The table below shows the optimal sizing of the recharging stations considering the events or contingencies (N - 1 and N - 2) generated in a geolocated area from the normal operating conditions (N - 0). These contingencies respond to the elimination of one or two recharge stations. In column 2 of Table 8, we show the CS that go out of service, and from columns 3 to 11, we present the flux density observed at each CS given a contingency. The out-of-service charging stations are randomly selected.

When considering the contingency analysis, the traffic density to meet the demand has to be reorganized and distributed with the enabled charging stations. Looking at column three of Table 8 under normal operating conditions, the vehicle density to be served by charging station ID 1 is $29.95 \approx 30$ vehicles in a time interval when the vehicle density is maximum. When the model experiences the departure from operation of the charging

Table 8

Case B: Optimal sizing of charging stations for EV based on multi-product flow problem.

Contingency	Deactivated (ID)	ID 1	ID 2	ID 3	ID 4	ID 5	ID 6	ID 7	ID 8	ID 9
N - 0	-	-3.00	-5.33	-4.84	-2.93	-2.18	-3.72	-3.55	-4.72	-4.62
N - 1	1	-	-5.60	-4.38	-4.97	-4.08	-3.90	-4.20	-4.16	-5.08
	2	-4.01	-	-5.98	-4.99	-3.65	-5.96	-4.48	-5.03	-4.93
	3	-4.27	-6.38	-	-3.62	-4.03	-4.56	-4.35	-5.11	-5.12
	4	-4.42	-4.32	-4.06	-	-3.55	-5.34	-4.72	-5.24	-5.68
	5	-4.41	-5.12	-4.81	-4.65	-	-5.24	-3.40	-5.48	-4.75
	6	-3.74	-4.37	-4.99	-6.05	-3.15	-	-4.34	-5.15	-5.79
	7	-4.25	-4.05	-5.31	-4.91	-3.53	-4.89	-	-5.53	-4.91
	8	-3.15	-4.98	-4.79	-4.73	-3.88	-5.12	-3.94	-	-4.85
	9	-4.02	-4.72	-5.41	-4.20	-3.35	-4.00	-4.86	-4.86	-
	Average (μ)	4,03	4,94	4,97	4,77	3,65	4,88	4,29	5,07	5,14
	Std. deviation (σ)	0,40	0,72	0,57	0,65	0,31	0,65	0,43	0,40	0,36
	$\mu + 2 * \sigma$	4,83	6,37	6,10	6,07	4,26	6,18	5,14	5,87	5,86
N - 2	1, 2	-	-	-4.67	-5.18	-4.89	-5.40	-5.54	-4.95	-5.42
	2, 3	-4.05	-	-	-4.25	-4.59	-5.42	-4.43	-6.08	-5.02
	8, 9	-4.13	-5.40	-5.49	-5.56	-5.12	-5.76	-5.46	-	-
	4, 5	-4.46	-4.89	-5.09	-	-	-6.08	-5.64	-5.71	-6.11
	7, 9	-4.83	-4.01	-7.10	-5.73	-4.31	-5.70	-	-5.93	-
	5, 7	-4.38	-4.20	-4.71	-4.25	-	-5.62	-	-6.31	-5.16
	3, 7	-5.37	-4.68	-	-5.09	-4.97	-5.13	-	-5.90	-6.14
	3, 5	-4.15	-5.03	-	-5.51	-	-4.95	-4.36	-5.80	-4.78
	2, 4	-5.20	-	-6.08	-	-5.22	-4.91	-5.06	-5.41	-6.00
	5, 6	-4.19	-4.94	-5.38	-6.36	-	-	-4.89	-6.11	-5.79
	7, 8	-4.30	-6.30	-4.50	-4.78	-5.27	-5.06	-	-	-5.46
	1, 3	-	-5.22	-	-4.25	-3.51	-5.89	-4.41	-5.69	-5.09
	3, 4	-4.77	-6.39	-	-	-3.84	-5.58	-5.07	-5.50	-6.08
	Average (μ)	4,53	5,11	5,38	5,10	4,64	5,46	4,98	5,76	5,55
	Std. deviation (σ)	0,43	0,74	0,81	0,68	0,59	0,36	0,47	0,36	0,47
	$\mu + 2 * \sigma$	5,39	6,58	7,00	6,46	5,82	6,19	5,93	6,48	6,50
Increment N - 1 (%)		61.0	19.5	26.0	107.2	95.4	66.1	44.8	24.4	26.8
Increment N - 2 (%)		79.7	23.5	44.6	120.5	167.0	66.4	67.0	37.3	40.7

station with ID 4, the thickness of vehicles to be served given the N - 1 contingency is 48.22 ≈ 48. If the charging infrastructure experiences the operation output of two CS with IDs 3 and 7 in contingency N - 2, the traffic density to be served is 53.81 ≈ 54 vehicles in a given time interval. Experience with the ID 1 charging station establishes that at N - 0, the vehicle density is three, with N - 1 and N - 2 at 4.83 and 5.39, respectively. This increase represents approximately 61% and 80% of the different traffic densities that will have to be served when the charging infrastructure disconnects the charging stations in the N - 1 and N - 2 contingencies, respectively. Likewise, we will perform the analysis for the recharging station with ID 5, which presents an increase in vehicle density of 95.4% in contingency N - 1 and an increase of 167.6% in contingency N - 2 have to be served if one or two recharging stations are disconnected.

It is understood as the algorithm reorganizing the vehicle flow based on a vector of cost and capacity for each road section, satisfying the mathematical variables of the linear equation. However, the equilibrium equations are satisfied for each iteration. If we pay attention to detail, the charging station with ID 5 in contingency N - 2 experiences increases in the density of vehicles that exceed 100% in the function of the regular operation in contingency N - 0. In addition, the increase in vehicular flow will depend on which charging station goes out of service.

Therefore, if the designer of the charging infrastructure knows what percentage would increase or decrease the vehicle density to be served by each CS, they can make intelligent decisions to foresee the electrical, civil, and logistic equipment necessary for the construction of charging infrastructures in electric mobility. Consequently, to determine the sizing of the CS, a rule of thumb is considered to find the magnitude of values. They are within a band around the mean in a normal distribution with twice the standard deviation width. Consequently, Table 8 with green indicates the maximum vehicular flow seen in each CS. The set of CS will result in the EV charging station infrastructure.

By multiplying the cumulative length in kilometers of the road network by the vehicle density, we can obtain the number of vehicles each CS should serve in each event studied. In addition, Table 9 allows us to verify by how much the sizing of the CS should increase given a circumstance. Consequently, the information presented so far is possible to plan the charging infrastructure for electric mobility in cities.

Up to this point, it has been possible to foresee the maximum number of vehicles that could enter each CS. Now, we proceed with the optimal sizing of charging terminals that a CS should have to meet the demand generated by EV operators. To this end, the following considerations will be made:

- The average charging time for 50 kW terminals is 30 min to reach 20–80%.
- The average charging time for 350 kW terminals will be 10 min to reach 20–80%.
- The optimal number of loading terminals is determined at 07:00 a.m. with the most vehicular traffic.

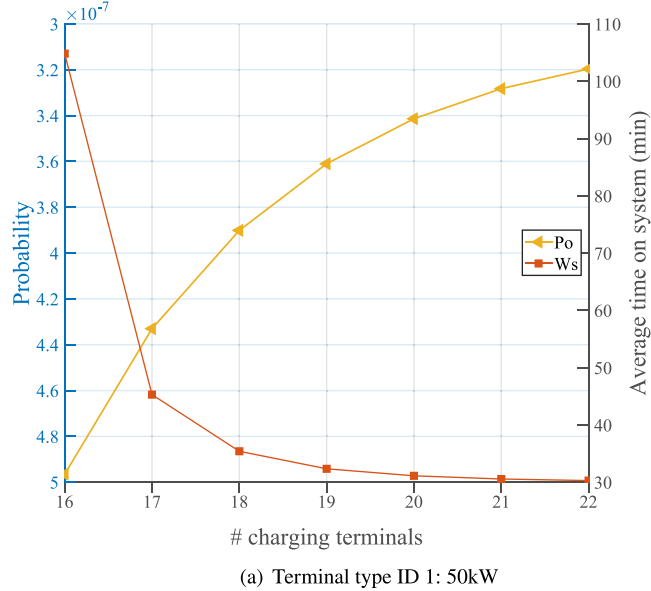
4.2.1. Optimum number of load terminals in case study B

With Fig. 13, the optimal number of charging terminals to be installed in the CS with ID 1 (see Table 9) in event N - 0 is presented. The metric in Fig. 13 illustrates that serving 30 EVs for 60 min requires 17 and 7 charging terminals with an output power of 50 kW and 350 kW, respectively. With this exciting data, it is possible to determine the installed capacity required in the CS with ID 1. Consequently, if it is necessary to establish a fast-charging infrastructure with 50 kW output power at each charging terminal, the installed capacity in the CS should be 850 kW. If the requirement in the infrastructure is ultra-fast charging terminals, the energy required in the CS should be 2.45 MW to cover the estimated demand during high vehicular traffic. Finally, an additional detail illustrated in Fig. 13 is the average time an electric vehicle remains in the system. Consequently, it

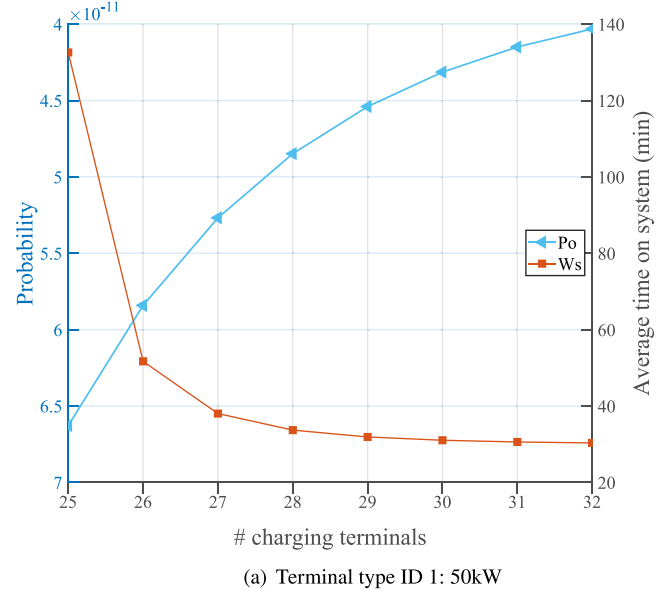
Table 9

Maximum partial demand at each charging station with 9,984 km of road network given a contingency.

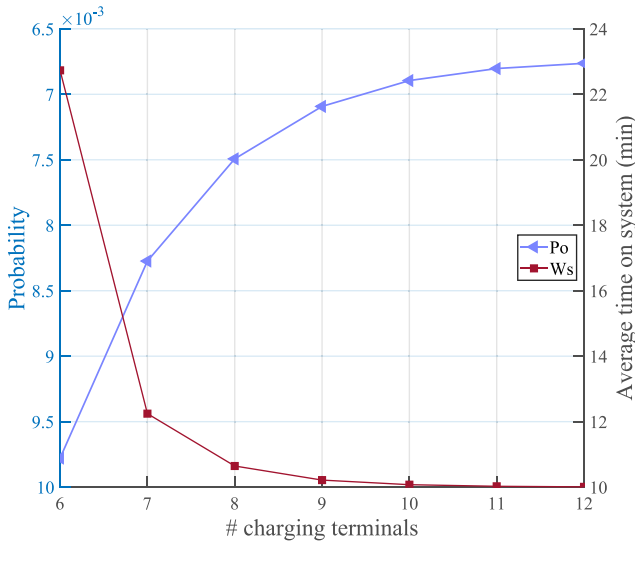
Events	ID 1	ID 2	ID 3	ID 4	ID 5	ID 6	ID 7	ID 8	ID 9
N - 0	30	53	48	29	22	37	35	47	46
N - 1	48	64	61	61	43	62	51	59	59
N - 2	54	66	70	65	58	62	59	64	65



(a) Terminal type ID 1: 50kW



(a) Terminal type ID 1: 50kW

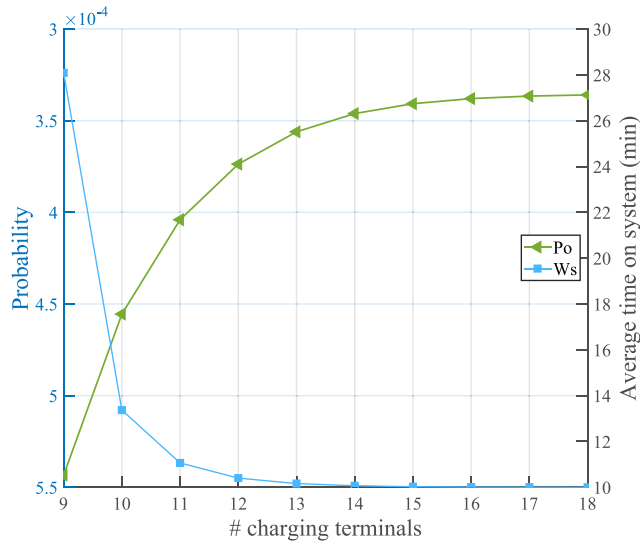


(b) Terminal type ID 1: 350kW

Fig. 13. Graphical method for determining the optimal number of load terminals with event $N - 0$.

is notorious for identifying that the higher the supply power at the charging terminals for battery recharging, the shorter the EV operator remains in the system.

Fig. 14 shows the optimal number of load terminals considering event $N - 1$. A reallocation of the number of terminals required to meet the demand when a CS goes out of the system's operation is evident. This reallocation is necessary because if a CS goes out of the process for any reason (preventive or corrective



(b) Terminal type ID 1: 350kW

Fig. 14. Graphical method to determine the optimal number of load terminals considering $N - 1$ event.

maintenance), the loading infrastructure is prepared to assume the demand that will no longer be covered by the CS that goes out of service. Consequently, with Fig. 14, the new number of charging terminals in $N - 1$ increases to 26 and 10 charging terminals with 50 kW and 350 kW output power at the service terminal, respectively. Consequently, the installed capacity in the CS for the different charging technologies is 1.3 MW and 3.5 MW, corresponding to an increase of 52.94% and 42.85%, respectively.

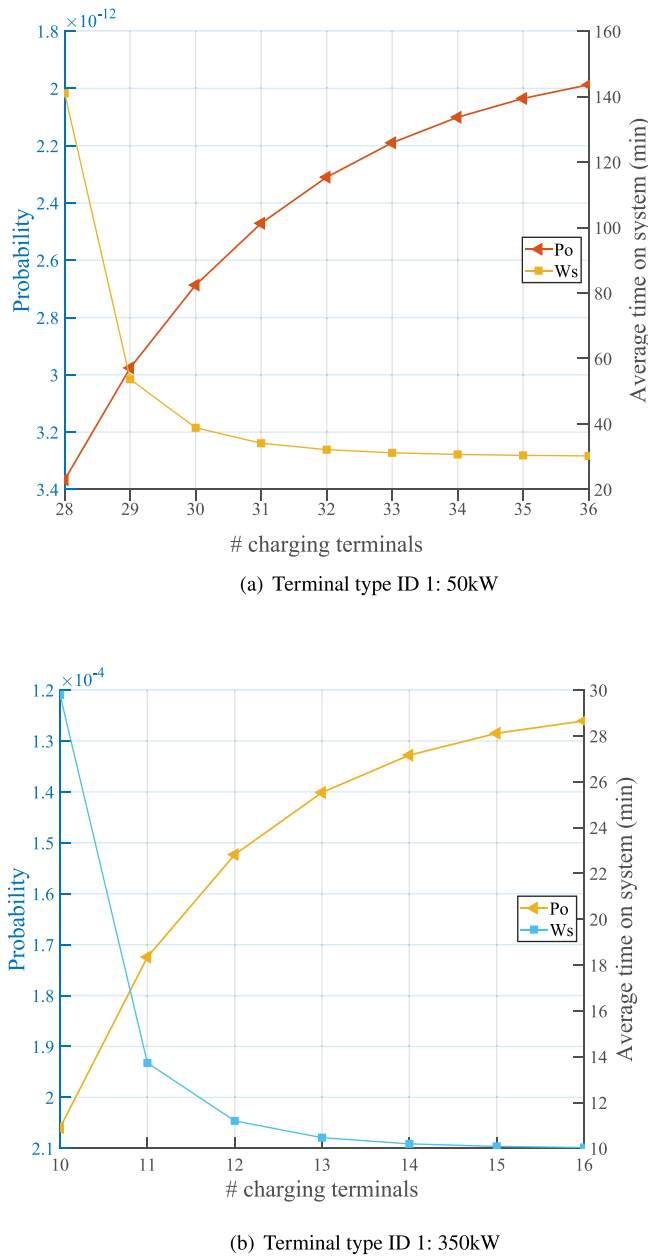


Fig. 15. Graphical method to determine the optimal number of load terminals considering $N - 2$ events.

Fig. 15 illustrates the number of charging terminals required to be installed in the CS with ID 1, considering the exit from the operation of two CS belonging to the charging infrastructure. Thus, it is evidenced that 29 and 11 charging terminals should be installed at the service station with ID 1 when two CS go out of operation. Consequently, the sizing for the CS with ID 1 is 1.45 MW and 3.85 MW for each type of technology, 50 kW and 350 kW, respectively.

The terminal charging technology directly relates to the supply power for battery recharging. Therefore, with **Figs. 13–15**, it is demonstrated that it is possible to determine the optimal number of charging terminals depending on the terminal charging technology to be considered in the CS by applying M/M/s queuing theory. In this case, 50 kW and 350 kW were used, which offer 30 and 10-minute charging times, respectively. Next, the graphical method will be applied to determine the number of terminals

Table 10

Charging infrastructure sizing applied to case study B with event $N - 1$ with 50 kW charging terminals.

Loading station	# Loading terminals	Total power (MW)
ID 1	26	1.30
ID 2	34	1.70
ID 3	32	1.60
ID 4	32	1.60
ID 5	23	1.15
ID 6	33	1.65
ID 7	27	1.35
ID 8	31	1.55
ID 9	31	1.55
Total		13.45

Table 11

Sizing of the loading infrastructure applied to case study B with event $N - 1$ with 350 kW loading terminals.

Loading Station	# Loading Terminals	Total power (MW)
ID 1	10	3.50
ID 2	12	4.20
ID 3	12	4.20
ID 4	12	4.20
ID 5	9	3.15
ID 6	12	4.20
ID 7	10	3.50
ID 8	11	3.85
ID 9	11	3.85
Total		34.65

required in each CS considering the output of a CS, which will give rise to the sizing of the EV charging infrastructure.

4.2.2. Optimal sizing of electrical equipment required in EV charging infrastructure

The number of charging terminals required in each CS is illustrated in **Tables 10** and **11** considering $N - 1$ events. **Table 10** shows the optimum number of charging terminals for electric vehicles weighing a charging time of 30 min from 20–80% charge. This type of terminal provides a service power of 50 kW. On the other hand, with **Table 11**, the charging time is 10 min with a terminal charging power of 350 kW. By purchasing the two tables, it is evidenced that the average installed power is 1.49 and 3.85 MW for fast and ultra-fast charging terminals, respectively. The average number of charging terminals with fast charging technology is 30 units, while for ultra-fast charging terminals, it is 11. On the other hand, the average time for the electric vehicle operator to remain in the system is 44 min with fast charging terminals and 18 min with ultra-fast charging terminals.

Therefore, the proposed model has demonstrated the ability to adapt to different case studies that allow us to analyze contingencies or events in the charging infrastructure, which are very useful when estimating the power installed in each CS. It will enable us to consider the electrical equipment, civil works, and logistics to construct adequately planned charging infrastructures.

The sizing and selection of the transformer for each CS are shown in **Table 12**. Based on the electrical power required to supply the demand and considering a safety factor of 25%, the transformer capacity to be installed is selected. Additional detail is that the final capacity of the transformer is chosen based on commercial transformers.

The CymDist software is used to determine the power flow of the loading infrastructure. **Fig. 16** illustrates the route to be followed by the primary feeder to the CS. The feeder route is constructed using a minimum-spanning tree. Consequently, it is ensured that the length of the conductor is the minimum required

Table 12
Sizing and selection of three-phase transformer for each charging station.

Loading station	Total power (MW)	Security factor 25% (MW)	Total power calculated (MVA)	Transformer 3 phases (MVA)
ID 1	1.30	1.63	1.65	2
ID 2	1.70	2.13	2.15	2.5
ID 3	1.60	2.00	2.02	2
ID 4	1.60	2.00	2.02	2
ID 5	1.15	1.44	1.46	2
ID 6	1.65	2.06	2.10	2.5
ID 7	1.35	1.69	1.71	2
ID 8	1.55	1.94	1.96	2
ID 9	1.55	1.94	1.96	2
Total	13.45	16.83	17.0	19

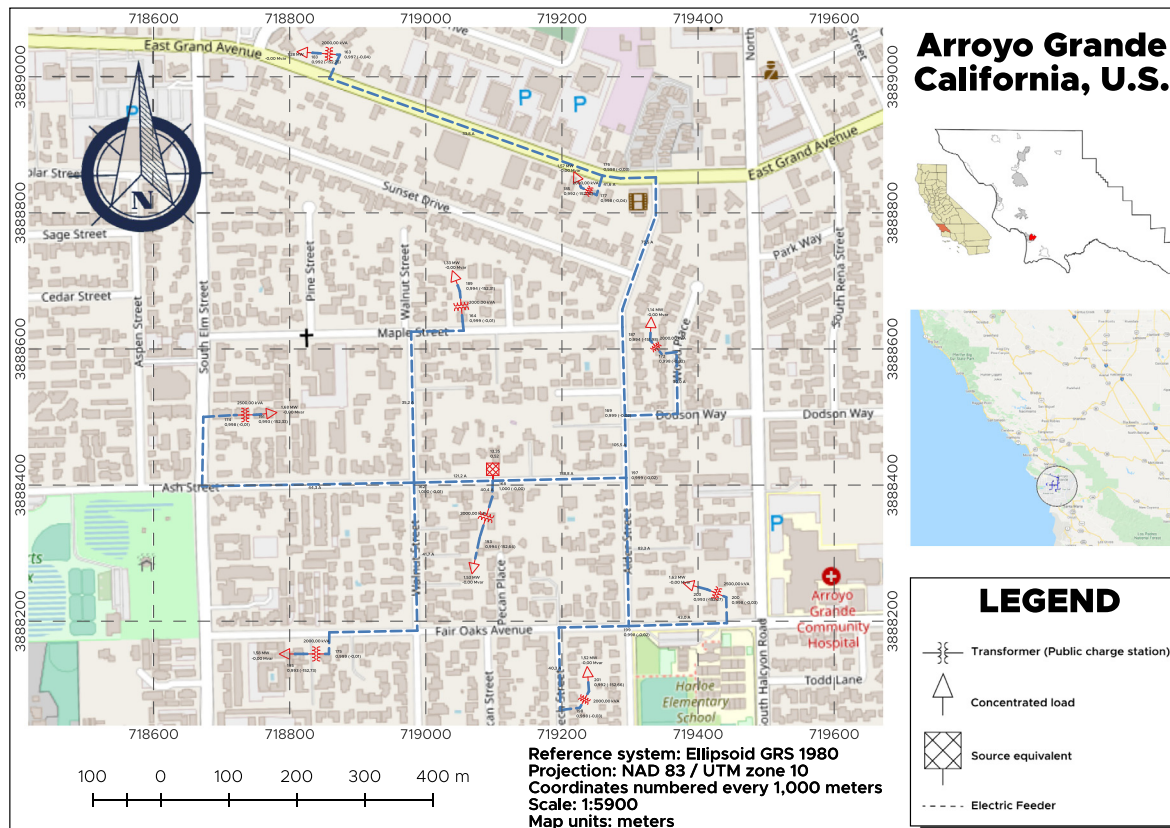


Fig. 16. Case B: Optimal routing of the primary feeder to the fast-charging stations.

to provide electrical power to each CS for EV. An additional detail shown with Fig. 16 is the load flow with power factor 0.99, transformer primary voltage 22 kV, and secondary voltage 480 V. Furthermore, a safety factor of 25% in addition to the installed power (see Table 10) is considered for transformer sizing.

With Table 13, you can see the different lengths of each conductor section. In addition, the maximum current flowing in the various areas of the primary feeder can be observed. The maximum current reflected in the source is 361.2 amperes. Another detail of interest shown in Table 13 is the losses in kW that occur due to the characteristics of the conductors and transformers. Consequently, with Table 13, it is possible to foresee the conductors required to construct the EV charging infrastructure.

The transformer's rated capacity, power throughput, total losses, and load percentage are illustrated in Table 14. The average chargeability of the transformer is approximately 70 percent, representing a 30 percent reserve, given that a commercial transformer is considered. Another detail of interest shown in Table 14 is the transformer's active and reactive power losses

caused by magnetization currents and by the characteristics of the conductor.

The average currents expected in the primary and secondary of the transformer installed in the different CS are 39 A and 1784 Amp, respectively, as shown in Table 15. The voltage drop from the source to the various nodes of the electrical circuit of the EV charging infrastructure is presented below.

Verifying that the voltage drop does not violate the admissible limits is essential. Fig. 17 shows the voltage drop from the source to each node energizing the transformer installed at each load station. Another detail observed is the conductors' length, i.e., at approximately 1200 meters from the source, the CS with ID 1 is located without violating the voltage drop limits.

Fig. 18 shows the total current THD as a function of frequency. Since this is a three-phase balanced system, harmonics 3, 5, 7, 9, and 11 average 9.404%. The average individual distortion factor (IHD) is 3.502%, so it is inferred that the limits indicated using the IEEE 519-1992 standard, where it is specified that for currents of $50 < 100$, the TDD 12% are not violated.

Table 13
Primary feeder power flow for fast charging terminals, 50 kW.

Node source	Node destination	Longitude (m)	Step power (kW)	Average PF (%)	Maximum current (A)	Losses (kW)	Charge %
167	168	25.7	1539.7	99.90	40.5	0.11	47.59
176	177	30.9	1581.1	99.89	41.6	0.14	48.98
197	169	91.2	4011.5	99.93	105.5	1.01	49.64
162	167	115.7	4615.8	99.93	121.2	1.70	57.04
199	200	182.1	1634.5	99.93	43.0	0.86	50.59
169	172	190.5	1141.3	99.95	30.0	0.44	35.31
167	197	196.1	7189.6	99.93	188.8	8.82	74.04
197	199	217.9	3169.2	99.92	83.3	1.52	39.22
199	198	252.6	1533.2	99.90	40.4	1.05	47.47
162	164	312.4	1341.3	99.96	35.2	0.50	22.40
162	175	378.4	1585.9	99.90	41.7	1.68	49.03
169	176	433.2	2869.2	99.93	75.5	2.47	35.51
162	174	458.0	1686.8	99.93	44.3	2.29	52.14
176	163	468.9	1285.7	99.94	33.8	1.37	39.81

Table 14
Power flow in transformers for fast charging terminals, 50 kW.

Charge Station	Nom Cap (kVA)	Step power (kW)	Primary Current (A)	Total losses (kW)	Total losses (kvar)	Charge (%)
ID 1	2000	1284.3	33,9	6,0	49,6	63,9
ID 2	2500	1684,6	44,3	7,8	68,0	67,1
ID 3	2000	1584,3	41,7	8,5	75,2	78,8
ID 4	2000	1580,9	41,6	8,5	75,1	78,6
ID 5	2000	1140,9	30,0	4,9	39,0	56,8
ID 6	2500	1633,7	43,0	7,4	64,0	65,1
ID 7	2000	1340,8	35,2	6,4	53,8	66,7
ID 8	2000	1539,6	40,5	8,1	70,8	76,6
ID 9	2000	1532,2	40,4	8,1	70,5	76,2

Table 15
Primary and secondary side transformer current.

Charging station	Primary (Amp)	Secondary (Amp)
ID 1	33.8	1550.0
ID 2	44.3	2030.2
ID 3	41.7	1909.3
ID 4	41.6	1907.1
ID 5	30.0	1374.4
ID 6	43.0	1969.7
ID 7	35.2	1614.0
ID 8	40.5	1852.8
ID 9	40.3	1848.1

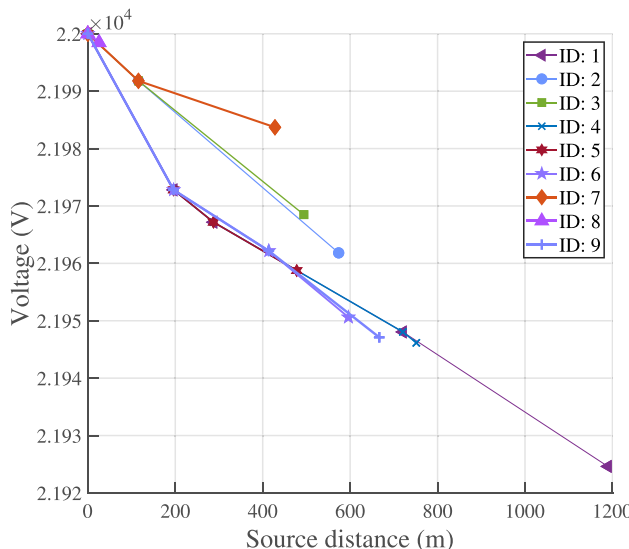


Fig. 17. Case B: Voltage drop from the source to the charging stations.

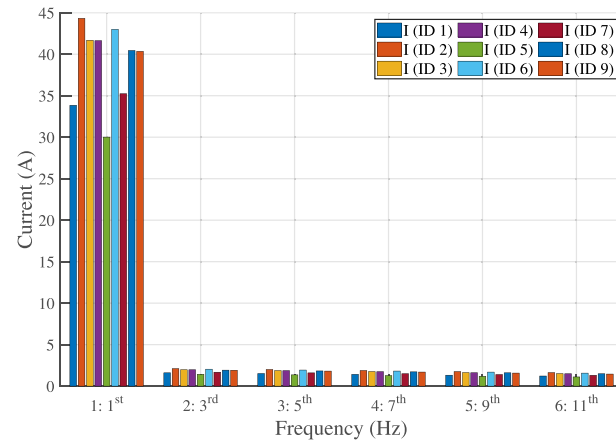


Fig. 18. Case B: Analysis of current vs. total frequency distortion in each CS.

The voltage distortion at the low voltage nodes as a function of time is presented in Fig. 19. If we compare it with Fig. 20, it can be identified that there is higher THD on the low voltage side. Another detail shown in Fig. 19 is the minimum voltage variation in each node serving the different charging stations. It is because the system analyzed is balanced since only the electrical network of the charging infrastructure is analyzed.

As viewed from the source, the THD is illustrated in Fig. 20. There is more significant distortion on the low voltage side of each of the transformers. This statement is contrasted with Table 16. There is a total distortion at the nodes connecting the primary and secondary sides of the transformer; also, the source is presented. The red color shows the nodes that violate the limits of the IEEE 519-1992 standard (see Table 16). Additional detail is that if Table 16 is evaluated with the IEEE 519-2014 standard,

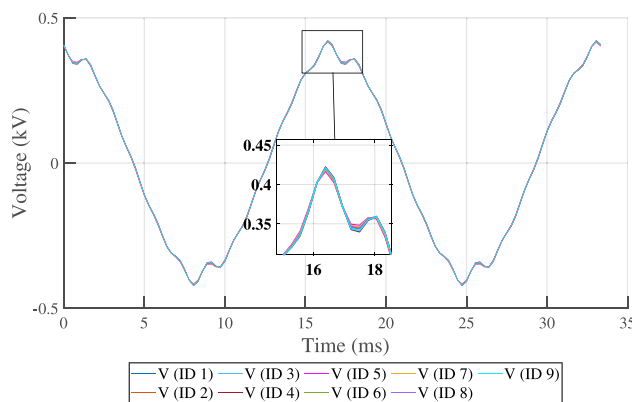


Fig. 19. Case B: Distortion analysis voltage vs. time in each CS node.

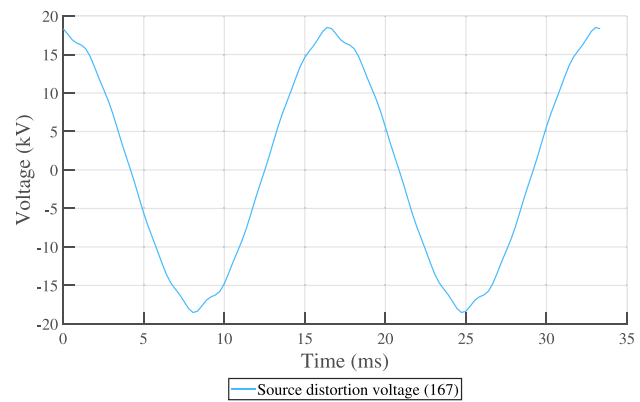


Fig. 20. Case B: Voltage vs. time distortion analysis at the source.

Table 16

Total harmonic voltage distortion at transformer and source nodes.

Charge station	Node (#)	HV (%)	LV (%)
ID 1	183	2.47	5.02
ID 2	191	2.18	4.88
ID 3	195	2.15	5.34
ID 4	185	2.40	5.55
ID 5	187	2.26	4.51
ID 6	203	2.31	4.92
ID 7	189	2.11	4.80
ID 8	193	2.01	5.11
ID 9	201	2.33	5.39
Source	167	2	

the established limits would not be violated. In the IEEE 519-1992 standard, a maximum THD of 5% is considered for voltages $\leq 1 \text{ kV}$. In the IEEE 519 - 2014 standard, 8% is considered for voltages $\leq 1 \text{ kV}$.

Consequently, the methodology proposed in this article has allowed the construction of the electrical network to energize the different CS that will serve multiple EV users. The proposed topology and sizing of the transformers have been simulated with CymDist software, validating the functionality of the proposed model. The importance of the simulation lies in verifying the operational performance of the charging infrastructure and thus being able to foresee corrective actions in favor of the charging infrastructure to be built.

5. Discussion

Implementing effective and efficient charging infrastructure is a crucial challenge to encourage the widespread use of electric vehicles and achieve a cleaner and more sustainable energy transition. Although the model proposed in this article provides a valuable contribution to the optimization of charging infrastructure resources, it is essential to consider the model's limitations and seek a more comprehensive and holistic approach to address this challenge.

In addition to the factors mentioned above, it is also necessary to consider regional differences in demand for electric vehicles and the availability of renewable energy resources, as this can significantly affect the location and size of charging stations. A more comprehensive approach that considers these considerations can help ensure that charging infrastructure is implemented fairly and equitably across regions, encouraging greater acceptance and adoption of electric vehicles nationwide.

6. Conclusions

This article has made planning EVCSI in geolocated scenarios possible based on free information from OpenStreetMap. This information contains the knowledge of the topology of the road network on which the case studies are analyzed.

With the proposed methodology, the maximum number of vehicles traveling on a given road network is predicted by observing its topology to allocate resources and size the EV charging infrastructure.

The heuristic has proven scalable and validated through case studies and iterative processes that address contingency concepts. Therefore, the main contribution of this work is its high potential to become a computational model and infrastructure manager for planning and resource allocation in electric mobility.

The heuristic provides finite and time-scalable solutions. The hourly analysis of vehicle flow has allowed identifying the maximum and minimum demands experienced by each CS, which contributes to coordinating and managing EV battery charging processes.

The CS sizing criteria are based on empirical statistical techniques, considering the mean with two standard deviations. Consequently, the M/M/s queuing system determines the optimal number of charging terminals.

Once the optimal number of charging terminals is found, the electrical equipment can be sized to meet the demand for battery recharging in electric mobility. In addition, the power flow study with load models is included to make a reading of the operation and functioning of the electrical network.

The study of harmonics, when modeling the load, becomes fundamental since power electronics are used in the load terminals. This study will allow foreseeing the necessary equipment with optimality criteria. Finally, this combinatorial problem needs more global solutions since its complexity increases exponentially as the topology grows.

CRediT authorship contribution statement

Miguel Campaña: Conceptualization, Methodology, Software, Formal analysis, Investigation, Writing – original draft, Writing – review & editing, Visualization. **Esteban Inga:** Conceptualization, Methodology, Validation, Writing – review & editing, Visualization, Supervision.

Declaration of competing interest

The authors declare that they have no known competing financial interests or personal relationships that could have appeared to influence the work reported in this paper.

Data availability

Data will be made available on request

Acknowledgments

This work was financially funded by the Smart Grid Research Group (GIREI) of Universidad Politécnica Salesiana, Ecuador (Project: Electric vehicle charging in buildings and its impact on the sizing and planning of electrical distribution networks) and the Power Grids and Smart Cities (RECI), Salesian Institutions of Higher Education (IUS).

References

- Amry, Y., Elbouchikhi, E., Le Gall, F., Ghogho, M., El Hani, S., 2022. Electric vehicle traction drives and charging station power electronics: Current status and challenges. *Energies* 15 (16), 1–30. <http://dx.doi.org/10.3390/en15166037>.
- Antarasee, P., Premrudeepreechacharn, S., Siritaratiwat, A., Khunkitti, S., 2023. Optimal design of electric vehicle fast-charging station's structure using metaheuristic algorithms. *Sustainability (Switzerland)* 15 (1), 22. <http://dx.doi.org/10.3390/su15010771>.
- Asna, M., Shareef, H., Prasanthi, A., 2023. Planning of fast charging stations with consideration of EV user, distribution network and station operation. *Energy Rep.* 9, 455–462. <http://dx.doi.org/10.1016/j.egyr.2023.01.063>.
- Azadi Moghaddam Arani, A., Jolai, F., Nasiri, M.M., 2019. A multi-commodity network flow model for railway capacity optimization in case of line blockage. *Int. J. Rail Transp.* 7 (4), 297–320. <http://dx.doi.org/10.1080/23248378.2019.1571450>.
- B, B.G., Ozlen, M., Neumann, F., 2018. Parallel Problem Solving from Nature - PPSN XV - 15th International Conference, Coimbra, Portugal, September 8–12, 2018, Proceedings, Part I. Vol. 1. Springer International Publishing, pp. 69–81. <http://dx.doi.org/10.1007/978-3-319-99253-2>.
- Balakrishna, P., Rajagopal, K., Swarup, K.S., 2014. AMI / GIS Based Distribution System Load Flow for Extended Situational Awareness. *IEEE*, pp. 1–6.
- Bevrani, B., Burdett, R.L., Bhaskar, A., Yarlagadda, P.K., 2019. A Multi Commodity Flow Model Incorporating Flow Reduction Functions. Springer US, <http://dx.doi.org/10.1007/s10696-019-09349-4>.
- Bi, X., Tang, W.K., 2019. Logistical planning for electric vehicles under time-dependent stochastic traffic. *IEEE Trans. Intell. Transp. Syst.* 20 (10), 3771–3781. <http://dx.doi.org/10.1109/TITS.2018.2883791>.
- Campaña, M., Inga, E., 2019a. Despliegue óptimo georreferenciado de estaciones de carga vehicular pública considerando capacidad de flujo y distancias máximas habilitantes. *I+D Tecnológico* 15 (2), 68–78. <http://dx.doi.org/10.33412/rd.v15.2.2248>.
- Campaña, M., Inga, E., 2019b. Heuristic method for optimal deployment of electric vehicle charge stations using linear programming. *Commun. Comput. Inf. Sci.* 1096 CCIS, 247–258. http://dx.doi.org/10.1007/978-3-030-36211-9_20.
- Campaña, M., Inga, E., 2019c. Optimal allocation of public charging stations based on traffic density in smart cities. In: 2019 IEEE Colombian Conference on Applications in Computational Intelligence, ColCACI 2019 - Proceedings. <http://dx.doi.org/10.1109/ColCACI.2019.8781986>.
- Campaña, M., Inga, E., Cárdenas, J., 2021. Optimal sizing of electric vehicle charging stations considering urban traffic flow for smart cities. *Energies* 14 (16), 1–16. <http://dx.doi.org/10.3390/en14164933>.
- Campaña, M., Inga, E., Hincapié, R., 2017. Optimal placement of universal data aggregation points for smart electric metering based on hybrid wireless. In: CEUR Workshop Proceedings. Vol. 1950. pp. 6–9.
- Chen, J., Chen, H., 2023. Stations considering user selection preferences. *Energies* 16 (4), <http://dx.doi.org/10.3390/en16041794>.
- Chung, B.D., Park, S., Kwon, C., 2018. Equitable distribution of recharging stations for electric vehicles. *Socio-Econ. Plan. Sci.* 63, 1–11. <http://dx.doi.org/10.1016/j.jseps.2017.06.002>.
- Demir, E., Huckle, K., Syntetos, A., Lahy, A., Wilson, M., 2019. Vehicle Routing Problem: Past and Future. Springer International Publishing, pp. 97–117. <http://dx.doi.org/10.1007/978-3-030-14493-7>.
- Du, L., Song, G., Wang, Y., Huang, J., Yu, Z., Ruan, M., 2018. Model for expressway network : A network flow approach. *IEEE Intell. Transp. Syst.* (January), 107–120. <http://dx.doi.org/10.1109/MITS.2017.2776130>.
- Esteban, I., Roberto, H., Sandra, C., 2019. Capacitated multicommodity flow problem for heterogeneous smart electricity metering communications using column generation. *Energies* 13 (1), 1–21. <http://dx.doi.org/10.3390/en13010097>.
- Gan, X., Zhang, H., Hang, G., Qin, Z., Jin, H., 2020. Fast charging station deployment considering elastic demand. *IEEE Trans. Transp. Electrif. PP (XX)*, 1. <http://dx.doi.org/10.1109/tte.2020.2964141>.
- Ghasemi, P., Khalili-Damghani, K., Hafezolkotob, A., Raissi, S., 2019. Uncertain multi-objective multi-commodity multi-period multi-vehicle location-allocation model for earthquake evacuation planning. *Appl. Math. Comput.* 350, 105–132. <http://dx.doi.org/10.1016/j.amc.2018.12.061>.
- Inga, E., Céspedes, S., Hincapié, R., Cárdenas, A., 2017. Scalable route map for advanced metering infrastructure based on optimal routing of wireless heterogeneous networks. *IEEE Wirel. Commun.* 24 (April), 1–8. <http://dx.doi.org/10.1109/MWC.2017.1600255>, URL <https://ieeexplore.ieee.org/document/7909154>.
- Inga, E., Hincapié, R., Céspedes, S., 2019. Capacitated multicommodity flow problem for heterogeneous smart electricity metering communications using column generation. *Energies* 13 (1), 1–21. <http://dx.doi.org/10.3390/en13010097>, URL <https://www.mdpi.com/1996-1073/13/1/97>.
- Jiang, J., Yue, Y., He, S., 2018. Multimodal-transport collaborative evacuation strategies for urban serious emergency incidents based on multi-sources spatiotemporal data. In: Leibniz International Proceedings in Informatics, LIPIcs. Vol. 114. No. 35. pp. 1–8. <http://dx.doi.org/10.4230/LIPIcs.GIScience.2018.35>.
- Jiménez-Estévez, G.A., Vargas, L.S., Marianov, V., 2010. Determination of feeder areas for the design of large distribution networks. *IEEE Trans. Power Deliv.* 25 (3), 1912–1922. <http://dx.doi.org/10.1109/TPWRD.2010.2042468>.
- Kłos, M.J., Sierpiński, G., 2023. Strategy for the siting of electric vehicle charging stations for parcel delivery service providers. *Energies* 16 (6), 2553. <http://dx.doi.org/10.3390/en16062553>.
- Konara, K.M.S.Y., Kolhe, M.L., Ulltveit-Moe, N., Balapuwaduge, I.A., 2023. Optimal utilization of charging resources of fast charging station with opportunistic electric vehicle users. *Batteries* 9 (2), <http://dx.doi.org/10.3390/batteries9020140>.
- Li, J., Ma, X.Y., Liu, C.C., Schneider, K.P., 2014. Distribution system restoration with microgrids using spanning tree search. *IEEE Trans. Power Syst.* 29 (6), 3021–3029. <http://dx.doi.org/10.1109/TPWRS.2014.2312424>.
- Liu, G., Kang, L., Luan, Z., Qiu, J., Zheng, F., 2019a. Charging station and power network planning for integrated electric vehicles (EVs). *Energies* 12 (13), 1–22. <http://dx.doi.org/10.3390/en12132595>.
- Liu, M., Richa, A.W., Rost, M., Schmid, S., 2019b. A constant approximation for maximum throughput multicommodity routing and its application to delay-tolerant network scheduling. In: Proceedings - IEEE INFOCOM. 2019-April. IEEE, pp. 46–54. <http://dx.doi.org/10.1109/INFOCOM.2019.8737402>.
- Lu, G., Zhou, X., Mahmoudi, M., Shi, T., Peng, Q., 2019. Optimizing resource recharging location-routing plans: A resource-space-time network modeling framework for railway locomotive refueling applications. *Comput. Ind. Eng.* 127, 1241–1258. <http://dx.doi.org/10.1016/j.cie.2018.03.015>.
- Luo, L., Wu, Z., Gu, W., Huang, H., Gao, S., Han, J., 2020. Coordinated allocation of distributed generation resources and electric vehicle charging stations in distribution systems with vehicle-to-grid interaction. *Energy* 192, <http://dx.doi.org/10.1016/j.energy.2019.116631>.
- Montoya, D.P., Ramirez, J.M., 2012. A minimal spanning tree algorithm for distribution networks configuration. In: IEEE Power and Energy Society General Meeting. pp. 1–7. <http://dx.doi.org/10.1109/PESGM.2012.6344718>.
- Moradipari, A., Alizadeh, M., 2018. Electric vehicle charging station network equilibrium models and pricing schemes. arXiv. [arXiv:1811.08582](http://arxiv.org/abs/1811.08582).
- Nagarajan, A., Ayyanar, R., 2014. Application of Minimum Spanning Tree Algorithm for Network Reduction of Distribution Systems. IEEE, pp. 1–5.
- Napolini, G., Polimeni, A., Micari, S., Andaloro, L., Antonucci, V., 2020. Optimal allocation of electric vehicle charging stations in a highway network: Part 1. Methodology and test application. *J. Energy Storage* 27 (October 2019), 101102. <http://dx.doi.org/10.1016/j.est.2019.101102>.
- Neagu, B.C., Georgescu, G., 2014. Wind farm cable route optimization using a simple approach. In: Electrical and Power Engineering (EPE), 2014 International Conference and Exposition on, Iasi. Vol. 1. No. Epe. pp. 1004–1009.
- Rabbani, M., Zenouzzadeh, S.M., Farrokhi-asl, H., 2019. Solving a bi-objective multi-commodity two-echelon capacitated location routing problem. *JISE* 12 (3), 249–268.
- Singh, P.P., Wen, F., Palu, I., Sachan, S., Deb, S., 2023. Electric vehicles charging infrastructure demand and deployment: Challenges and solutions. *Energies* 16 (1), <http://dx.doi.org/10.3390/en16010007>.

- Song, D., Tharmarasa, R., Zhou, G., Florea, M.C., Duclos-Hindie, N., Kirubarajan, T., 2019. Multi-vehicle tracking using microscopic traffic models. *IEEE Trans. Intell. Transp. Syst.* 20 (1), 149–161. <http://dx.doi.org/10.1109/TITS.2018.2804894>.
- Tang, X., Bi, S., Zhang, Y.-J.A., 2018. Distributed routing and charging scheduling optimization for internet of electric vehicles. *IEEE Internet Things J.* PP (c), 1. <http://dx.doi.org/10.1109/JIOT.2018.2876004>, URL <https://ieeexplore.ieee.org/document/8491301/>.
- Tian, H., Tzelepis, D., Papadopoulos, P.N., 2021. Electric vehicle charger static and dynamic modelling for power system studies. *Energies* 14 (7), <http://dx.doi.org/10.3390/en14071801>.
- Vaziri, S., Etebari, F., Vahdani, B., 2019. Development and optimization of a horizontal carrier collaboration vehicle routing model with multi-commodity request allocation. *J. Clean. Prod.* 224, 492–505. <http://dx.doi.org/10.1016/j.jclepro.2019.02.043>.
- Zhang, Y., Ioannou, P.A., 2018. Integrated control of highway traffic flow. *J. Control Decis.* 5 (1), 19–41. <http://dx.doi.org/10.1080/23307706.2017.1402715>.
- Zhang, X., Rey, D., Waller, S.T., Chen, N., 2019. Range-constrained traffic assignment with multi-modal recharge for electric vehicles. *Netw. Spat. Econ.* 19 (2), 633–668. <http://dx.doi.org/10.1007/s11067-019-09454-9>.